

Predicting the Clustering of X-Ray Selected Galaxy Clusters in Flux-Limited Surveys

L. Moscardini¹, S. Matarrese^{2,3}, F. Lucchin¹ and P. Rosati⁴

¹*Dipartimento di Astronomia, Università di Padova, vicolo dell'Osservatorio 5, I-35122 Padova, Italy*

²*Dipartimento di Fisica G. Galilei, Università di Padova, via Marzolo 8, I-35131 Padova, Italy*

³*Max-Planck-Institut für Astrophysik, Karl-Schwarzschild-Strasse 1, D-85748 Garching, Germany*

⁴*ESO – European Southern Observatory, Karl-Schwarzschild-Strasse 2, D-85748 Garching, Germany*

26 April 2024

ABSTRACT

We present a model to predict the clustering properties of X-ray selected clusters in flux-limited surveys. Our technique correctly accounts for past light-cone effects on the observed clustering and follows the non-linear evolution in redshift of the underlying dark matter correlation function and cluster bias factor. The conversion of the limiting flux of a survey into the corresponding minimum mass of the hosting dark matter haloes is obtained by using theoretical and empirical relations between mass, temperature and X-ray luminosity of galaxy clusters. Finally, our model is calibrated to reproduce the observed cluster counts adopting a temperature-luminosity relation moderately evolving with redshift. We apply our technique to three existing catalogues: the ROSAT Brightest Cluster sample (BCS); the X-ray brightest Abell-type cluster sample (XBACs); the ROSAT-ESO Flux Limited X-ray sample (REFLEX). Moreover, we consider an example of possible future space missions with fainter limiting flux. In general, we find that the amplitude of the spatial correlation function is a decreasing function of the limiting flux and that the Einstein-de Sitter models always give smaller correlation amplitudes than open or flat models with low matter density parameter Ω_{0m} . In the case of the XBACs catalogue, the comparison with previous estimates of the observational spatial correlation shows that only the predictions of models with $\Omega_{0m} = 0.3$ are in good agreement with the data, while the Einstein-de Sitter models have too low a correlation strength. Finally, we use our technique to discuss the best strategy for future surveys. Our results show that to study the clustering properties of X-ray selected clusters the choice of a wide area catalogue, even with a brighter limiting flux, is preferable to a deeper, but with smaller area, survey.

Key words: cosmology: theory – galaxies: clusters – large-scale structure of Universe – X-rays: galaxies – dark matter

1 INTRODUCTION

Extending the study of the matter distribution to the largest scales reachable by observations can provide important constraints on models for the formation of cosmic structures. In fact, on very large scales the present-day fluctuation field is just a linear amplification of the primordial one. In the past years, surveys of galaxies have been used to describe the spatial distribution of the cosmic structures up to few hundred Mpc. It is now well established that an accurate and efficient alternative way to describe the very large scale structure of the universe is to use the spatial distribution of clusters of galaxies. In the framework of the gravitational instability picture galaxy clusters are the most extended gravitationally bound systems in the universe. Moreover, their typical separation is much larger than their expected displacements from the primordial positions. Therefore, their study can be quite useful in putting constraints on the cosmological parameters. This possibility is made easier by the fact that the cluster clustering

signal is enhanced with respect to the galaxy one, because the clusters are expected to form in highly overdense regions (peaks) of the cosmological density field and are consequently strongly biased (Kaiser 1984).

For all these reasons, a large effort has been made to compile cluster surveys, leading to extended redshift catalogues in the optical band (see e.g. Postman 1998 for a review). However, as first suggested by Sutherland (1988), this kind of catalogues can be affected by strong problems due to the spurious presence of interloper galaxies, which would alter the general statistical properties of the clusters. This problem does not affect surveys obtained in the X-ray band, where the cluster emission, due to the thermal bremsstrahlung originated in the hot intracluster plasma, is more concentrated around the centre, because of its dependence on the square of the baryonic density. In the last twenty years, various space missions have been planned (and launched) to build extended catalogues of X-ray selected clusters. To this aim the role played by the ROSAT satellite has been quite important. From its all-sky survey, which was carried out in the soft (0.1–2.4 keV) X-ray band, different catalogues of clusters have been built: the RASS1 Bright sample (De Grandi et al. 1999a), the BCS sample (Ebeling et al. 1998), the XBACs sample (Ebeling et al. 1996) and the REFLEX sample (Böhringer et al. 1998); more details about these surveys can be found in Section 4.1. These data have been essentially used to compute the cluster number counts and the X-ray luminosity function, which have relevant cosmological implications. In particular, the analysis of the cluster abundance (also as a function of redshift) has been largely used to provide estimates of the mass fluctuation amplitude and of the matter density parameter Ω_{m} (e.g. Eke, Cole & Frenk 1996; Viana & Liddle 1996; Mo, Jing & White 1996; Oukbir, Bartlett & Blanchard 1997; Eke et al. 1998; Sadat, Blanchard & Oukbir 1998; Viana & Liddle 1999; Borgani, Plionis & Kolokotronis 1999; Borgani et al. 1999).

An alternative approach is based on the study of the spatial distribution of X-ray selected clusters. The standard statistical tools used to this aim are the (spatial and angular) two-point correlation function and the power-spectrum. Pioneering studies on small samples have been performed by Lahav et al. (1989), Nichol, Briel & Henry (1994) and Romer et al. (1994), suggesting relatively small values of the correlation length r_0 . In particular Romer et al. (1994) found $r_0 = 13\text{--}15 h^{-1}$ Mpc (h is the value of the local Hubble constant H_0 in units of $100 \text{ km s}^{-1} \text{ Mpc}^{-1}$) by analysing a sample of galaxy clusters selected from the ROSAT All-Sky Survey. Very recently the amount of data has become large enough to allow more reliable estimates of the spatial correlation function $\xi(r)$. For example, Abadi, Lambas & Muriel (1998) and Borgani, Plionis & Kolokotronis (1999) analysed the XBACs catalogue obtaining correlation lengths in the range $r_0 \approx 20\text{--}26 h^{-1}$ Mpc, while Moscardini et al. (2000) found $r_0 = 21.5^{+3.4}_{-4.4} h^{-1}$ Mpc using the RASS1 Bright Sample. Notice that these values are larger than the correlation amplitudes ($r_0 \approx 13\text{--}18 h^{-1}$ Mpc) resulting from the optical data, once corrected for the previously quoted projection effects (see e.g. the APM analysis performed by Croft et al. 1997). In the near future, with the new generation of X-ray satellites, such as XMM and Chandra, the quality and quantity of the cluster data will sensibly increase, giving the opportunity to improve the clustering measurements and to better understand the reasons for this difference.

In this paper we introduce a theoretical model to make predictions on the correlations of X-ray selected clusters in flux-limited surveys. The method, which fully accounts for the past light-cone effects using a technique developed in Matarrese et al. (1997) and Moscardini et al. (1998), also takes into account the non-linear growth of clustering and the redshift evolution of the cluster bias factor. The conversion of the limiting flux of a given survey into the corresponding mass of the hosting dark matter haloes is made by using theoretical and empirical relations between mass, temperature and X-ray luminosity of galaxy clusters. The same method described here has been already applied in Moscardini et al. (2000), where a comparison between observational results and theoretical predictions for the RASS1 Bright Sample has been performed. A similar approach (which, however, neglects the past light-cone effects and the non-linear evolution of clustering) has been adopted by Borgani, Plionis & Kolokotronis (1999) in their analysis of the XBACs catalogue. Suto et al. (2000) made quantitative predictions for future surveys adopting a very similar method, using an equivalent formalism to allow for past light-cone effects, but also including a model for the redshift-space distortions.

The plan of the paper is as follows. In Section 2 we discuss our method to study the clustering of a class of objects in the past light-cone and present the relevant formulas for the (spatial and angular) two-point correlation and for the power-spectrum. In Section 3 we introduce our theoretical model to estimate the correlations of X-ray selected clusters. In particular, we discuss how to follow the redshift evolution of the cluster bias and of the mass auto-correlation function and how to convert the catalogue limiting flux into a minimum halo mass. The different cosmological scenarios here considered and the resulting X-ray cluster number counts are also presented. Section 4 is devoted to the theoretical predictions of the clustering properties for various present and future catalogues. Section 5 presents a discussion of the robustness of the results with respect to different choices of the parameters. Conclusions are drawn in Section 6.

2 CLUSTERING IN THE PAST LIGHT-CONE

2.1 Spatial two-point function

Our aim is to obtain theoretical expectations for the correlation properties of high-redshift objects like galaxies, clusters, etc. Let us start by defining $n_{\text{obs}}(r(z)\hat{\gamma}; z, M)$ as the number of objects with redshift z that an observer placed in the origin measures in the angular direction specified by the unit vector $\hat{\gamma}$, per unit comoving volume and per unit logarithmic interval of some set of intrinsic properties (like mass, luminosity, etc.), generally denoted by M . Here $r(z)$ is the comoving radial distance related to the redshift z via the general law (the effect of peculiar velocities on the redshift-distance relation is here disregarded)

$$r(z) = \frac{c}{H_0 \sqrt{|\Omega_{0\mathcal{R}}|}} \mathcal{S} \left(\sqrt{|\Omega_{0\mathcal{R}}|} \int_0^z \frac{dz'}{E(z')} \right), \quad (1)$$

where (e.g. Peebles 1993)

$$E(z) \equiv H(z)/H_0 = [\Omega_{0\text{m}}(1+z)^3 + \Omega_{0\mathcal{R}}(1+z)^2 + \Omega_{0\Lambda}]^{1/2}, \quad (2)$$

and $\Omega_{0\mathcal{R}} \equiv 1 - \Omega_{0\text{m}} - \Omega_{0\Lambda}$ with $\Omega_{0\text{m}}$ and $\Omega_{0\Lambda}$ the present density parameters for the non-relativistic matter and cosmological constant components, respectively. In the above formula, for an open universe model, $\Omega_{0\mathcal{R}} > 0$, $\mathcal{S}(x) \equiv \sinh(x)$, for a closed universe, $\Omega_{0\mathcal{R}} < 0$, $\mathcal{S}(x) \equiv \sin(x)$, while in the Einstein-de Sitter case, $\Omega_{0\mathcal{R}} = 0$, $\mathcal{S}(x) \equiv x$. In what follows we will also need the Jacobian determinant

$$g(z) \equiv r^2(z) \left[1 + \frac{H_0^2}{c^2} \Omega_{0\mathcal{R}} r^2(z) \right]^{-1/2} \frac{dr}{dz}. \quad (3)$$

To obtain an expression for the two-point correlation function, we start by writing the average number of distinct pairs with relative separation in the range $r, r+dr$, with redshift in the range \mathcal{Z} and M in the domain \mathcal{M} . This reads

$$\begin{aligned} \langle N_{\text{pairs}}(r) \rangle dr &= \frac{1}{2} \int_{\mathcal{M}} d \ln M_1 d \ln M_2 \int_{\mathcal{Z}} dz_1 dz_2 g(z_1) g(z_2) \times \\ &\int_{4\pi} d\Omega_{\gamma_1} d\Omega_{\gamma_2} \delta^D(r - |r_1 \hat{\gamma}_1 - r_2 \hat{\gamma}_2|) \langle n_{\text{obs}}(r(z_1)\hat{\gamma}_1; z_1, M_1) n_{\text{obs}}(r(z_2)\hat{\gamma}_2; z_2, M_2) \rangle dr, \end{aligned} \quad (4)$$

where δ^D is the Dirac delta function. One can transform the above delta function into a delta function over the relative angular separation [accounting for the Jacobian $r/(r_1 r_2)$], integrate over the angles and then proceed as in Matarrese et al. (1997) [see the discussion after eq.(11)]. In such a calculation one can safely neglect curvature corrections to the cosine rule, which would in principle arise whenever $\Omega_{0\mathcal{R}} \neq 0$ (see in this respect the discussion in Matarrese et al. 1997). The result is the exact expression

$$\langle N_{\text{pairs}}(r) \rangle dr = \frac{1}{2} \int_{\mathcal{Z}} dz_1 dz_2 \frac{\mathcal{N}(z_1)}{r(z_1)} \frac{\mathcal{N}(z_2)}{r(z_2)} \left[1 + \xi_{\text{obj}}(r; z_1, z_2) \right] r dr, \quad (5)$$

where $\xi_{\text{obj}}(r; z_1, z_2)$ is the theoretical correlation function of the given objects at separation r and redshifts z_1, z_2 , integrated over the domain of M values. Here $\mathcal{N}(z)$ is the actual redshift distribution of the catalogue, which is given by $\mathcal{N}(z) = \int_{\mathcal{M}} d \ln M \mathcal{N}(z, M)$, with $\mathcal{N}(z, M) = 4\pi g(z) \phi(z, M) \bar{n}(z, M)$, where $\bar{n}(z, M)$ is the expected number of objects per comoving volume at redshift z and $\phi(z, M)$ the isotropic catalogue selection function, which also accounts for possible incomplete sky-coverage, as a function of redshift and object intrinsic properties.

A somewhat simpler formula can be obtained by using the delta function to integrate over one redshift and by making the following two *approximations*: i) the redshift distribution $\mathcal{N}(z)$ is almost constant over redshift intervals corresponding to the considered comoving separation r , ii) the theoretical correlation does not change considerably over the time intervals corresponding to the separation r . The resulting expression for the mean number of pairs reads

$$\langle N_{\text{pairs}}(r) \rangle dr = \frac{1}{2} \int_{\mathcal{Z}} dz \frac{\mathcal{N}^2(z)}{g(z)} \left[1 + \xi_{\text{obj}}(r; z) \right] r^2 dr. \quad (6)$$

We therefore get two alternative expressions for the correlation function: using eq.(5) above we find

$$\xi_{\text{obs}}(r) = \frac{\int_{\mathcal{Z}} dz_1 dz_2 \mathcal{N}(z_1) r^{-1}(z_1) \mathcal{N}(z_2) r^{-1}(z_2) \xi_{\text{obj}}(r; z_1, z_2)}{\left[\int_{\mathcal{Z}} dz_1 \mathcal{N}(z_1) r^{-1}(z_1) \right]^2}, \quad (7)$$

[which differs from eq.(15) of Matarrese et al. (1997), by the extra factors $1/r(z)$ in the redshift integrations], while using eq.(6) we obtain the approximate formula

$$\xi_{\text{obs}}(r) = \frac{\int_{\mathcal{Z}} dz_1 \mathcal{N}^2(z_1) g^{-1}(z_1) \xi_{\text{obj}}(r; z_1)}{\int_{\mathcal{Z}} dz_1 \mathcal{N}^2(z_1) g^{-1}(z_1)}. \quad (8)$$

The latter expression has been independently derived by Yamamoto & Suto (1999).

Note that compared to eq.(15) of Matarrese et al. (1997) these expressions give larger weight to lower redshift pairs. Nevertheless, these pairs are also preferred by the selection function, so, one might argue that the change implied is generally small. Similar conclusions have been reached by Yamamoto & Suto (1999). More in general, one might introduce some weight $w(z)$ in the redshift integrations in order to maximize the signal for the correlation function, as suggested by Matsubara, Suto & Szapudi (1997). In this sense eq.(7) above and eq.(15) in (Matarrese et al. 1997), correspond to different choices for the weight. In what follows we will adopt the exact expression in eq.(7) for the correlation function. The problems related to the presence of a double redshift dependence of the intrinsic object correlation in eq.(7) will be dealt with by replacing z_1 and z_2 with a suitable average redshift z_{ave} . Following Porciani (1997) we choose z_{ave} so that the linear growth factor of density fluctuations $D_+(z_{\text{ave}})$ equals the geometric mean of $D_+(z_1)$ and $D_+(z_2)$; this is expected to give an accurate approximation to the exact formula, even on mildly non-linear scales.

In our treatment we disregard the effect of redshift-space distortions. Analytical expressions have been obtained in the mildly non-linear regime, by using either the Zel'dovich approximation (Fisher & Nusser 1996; Taylor & Hamilton 1996; Hui, Kofman & Shandarin 1999) or higher order perturbation theory (Heavens, Matarrese & Verde 1998). The complicating role of the cosmological redshift-space distortions on the evolution of the bias factor has been considered by Suto et al. (1999,2000). Recently, Nishioka & Yamamoto (1999) have examined the redshift-space distortions effects on the two-point correlation function and power-spectrum of high-redshift objects; Magira, Jing & Suto (2000) have extended the formalism to account for the non-linear effects of the density and velocity evolution. Suto et al. (2000), in a general study of the two-point function of X-ray selected clusters, have included the effect of both linear and non-linear redshift-space distortions. An estimate of the effect of large-scale redshift-space distortions can be obtained within linear theory and the distant-observer approximation (Kaiser 1987; see Zaroubi & Hoffman 1996 and Matsubara 1999 for an extension of this formalism to all-sky surveys). In this case the enhancement of the redshift-space averaged power-spectrum is given by the factor $1 + 2\beta(z)/3 + \beta^2(z)/5$, where $\beta(z) = f(z)/b_{\text{eff}}(z)$. In the previous expression $f \equiv -d \ln D_+(z)/d \ln(1+z) \simeq \Omega_m^{0.6}(z) + \Omega_\Lambda(z)[1 + \Omega_m(z)/2]/70$ (Lahav et al. 1991) and $b_{\text{eff}}(z)$ is the effective bias (see below). Plionis & Kolokotronis (1998), by analysing the XBACs catalogue and using linear perturbation theory to relate the X-ray cluster dipole to the Local Group peculiar velocity, found $\beta \simeq 0.24 \pm 0.05$. Adopting this approach, Borgani, Plionis & Kolokotronis (1999) conclude that the overall effect of redshift-space distortions is a small change of the correlation function, which expressed in terms of r_0 corresponds to an $\simeq 8$ per cent increase. For deeper surveys, such as ABRIXAS (see below) the linear redshift-space distortion becomes slightly smaller (approximately 6 per cent increase of the correlation length), because of the b_{eff} increase with redshift.

2.2 Power-spectrum

The exact formula for the power-spectrum is given by the Fourier transform of eq.(7) above. However, an even simpler expression can be obtained by Fourier transforming eq.(8):

$$P_{\text{obs}}(k) = \frac{\int_{\mathcal{Z}} dz \mathcal{N}^2(z) g^{-1}(z) P_{\text{obj}}(k; z)}{\int_{\mathcal{Z}} dz \mathcal{N}^2(z) g^{-1}(z)}. \quad (9)$$

Quite recently, Yamamoto, Nishioka & Suto (1999) have performed a detailed and rigorous study of light-cone effects on the power-spectrum. It turns out that our expression in eq.(9) reduces to the approximate formula in their eq.(16) on linear scales. As Yamamoto, Nishioka & Suto (1999) show, this simple expression is accurate for wave-numbers $k \gg 1/r(z_{\text{max}})$, where $r(z_{\text{max}})$ is the maximum redshift of the considered survey.

2.3 Angular two-point function

The angular correlation function $\omega_{\text{obs}}(\vartheta)$ is easily obtained in a similar way. The number of pairs with relative angular separation ϑ is defined similarly to eq.(4), where, however, the delta function over the radial distances is replaced by one over directions in the sky, namely $\delta^D(\hat{\gamma}_1 \cdot \hat{\gamma}_2 - \cos \vartheta)$. Integrating over all the angles one obtains

$$\omega_{\text{obs}}(\vartheta) = N^{-2} \int_{\mathcal{Z}} dz_1 dz_2 \mathcal{N}(z_1) \mathcal{N}(z_2) \xi_{\text{obj}}(r_{12}; z_1, z_2), \quad r_{12} = \sqrt{r^2(z_1) + r^2(z_2) - 2r(z_1)r(z_2)\cos \vartheta}, \quad (10)$$

having once again neglected curvature corrections to the cosine rule. Adopting then the *small-angle* approximation (e.g. Peebles 1980) one gets the simpler expression

$$\omega_{\text{obs}}(\vartheta) = N^{-2} \int_{\mathcal{Z}} dz \left(\frac{dr}{dz} \right)^{-1} \mathcal{N}^2(z) \int_{-\infty}^{\infty} du \xi_{\text{obj}}[r(u, \vartheta, z), z], \quad (11)$$

with $r(u, \vartheta, z) = \sqrt{u^2 + r^2(z)\vartheta^2}$.

3 MODELLING THE TWO-POINT FUNCTION OF X-RAY CLUSTERS

3.1 The effective bias of galaxy clusters

To proceed in our modelling, we can safely assume that X-ray clusters are in a one-to-one relation with virialized dark matter haloes and take a linear bias model (see, however, Catelan et al. 1998 and Catelan, Matarrese & Porciani 1998, for a more refined bias prescription), namely $\delta_{\text{cl}}(\mathbf{x}; M, z) \simeq b(M, z)\delta_{\text{m}}(\mathbf{x}, z)$, where M is now the halo mass and z the considered redshift. As a consequence we can write the object two-point function as being proportional to the mass auto-correlation function, namely $\xi_{\text{obj}}(r; z_1, z_2) \approx b_{\text{eff}}(z_1)b_{\text{eff}}(z_2)\xi(r, z_1, z_2)$. Here, following Matarrese et al. (1997), we introduced the *effective bias* factor

$$b_{\text{eff}}(z) \equiv \mathcal{N}^{-1}(z) \int_{\mathcal{M}} d \ln M' b(M', z) \mathcal{N}(z, M'). \quad (12)$$

The assumption of a linear bias, as above, allows to further simplify our expressions for correlation functions and power-spectrum. We get

$$\xi_{\text{obs}}(r) = \frac{\int_{\mathcal{Z}} dz_1 dz_2 \mathcal{N}(z_1) r^{-1}(z_1) b_{\text{eff}}(z_1) \mathcal{N}(z_2) r^{-1}(z_2) b_{\text{eff}}(z_2) \xi(r; z_{\text{ave}})}{\left[\int_{\mathcal{Z}} dz_1 \mathcal{N}(z_1) r^{-1}(z_1) \right]^2}, \quad (13)$$

for the spatial two-point function,

$$P_{\text{obs}}(k) = \frac{\int_{\mathcal{Z}} dz \mathcal{N}^2(z) g^{-1}(z) b_{\text{eff}}^2(z) P(k; z)}{\int_{\mathcal{Z}} dz \mathcal{N}^2(z) g^{-1}(z)}, \quad (14)$$

for the power-spectrum, and

$$\omega_{\text{obs}}(\vartheta) = N^{-2} \int_{\mathcal{Z}} dz \left(\frac{dr}{dz} \right)^{-1} \mathcal{N}^2(z) b_{\text{eff}}^2(z) \int_{-\infty}^{\infty} du \xi[r(u, \vartheta, z), z], \quad (15)$$

for the angular two-point function, which coincides with eq.(20) in Matarrese et al. (1997).

In order to predict the clustering properties of our X-ray clusters as a function of redshift we need to understand how the relation between these objects and the underlying mass distribution evolves in time, i.e. how the effective bias evolves. For the cluster population it is extremely reasonable to assume that structures on a given mass scale are formed by the hierarchical merging of smaller mass units; for this reason we can consider clusters as being fully characterized at each redshift z by the mass M and formation epoch z_f of their hosting dark matter haloes. For cluster-size haloes it is safe to assume that instantaneous merging operates, so that $z_f = z$ [see, e.g., the discussion in Kravtsov & Klypin (1999); the effect of taking $z \neq z_f$ in $\Omega_{\text{om}} < 1$ models has been discussed by various authors (Kitayama & Suto 1996; Viana & Liddle 1996; Voit & Donahue 1998)]. In this way their comoving mass function $\bar{n}(z, M)$ can be computed using an approach derived from the Press-Schechter (1974) technique. Moreover, it is possible to adopt for the ‘monochromatic’ bias $b(M, z)$ the expression which holds for virialized dark matter haloes (e.g. Mo & White 1996; Catelan et al. 1998). Recently, a number of authors (e.g. Sheth & Tormen 1999 and references therein) have shown that the Press-Schechter relation does not provide an accurate description of the halo abundance both in the small-mass tail and in the large-mass one, which is more relevant for the present study. Also, the simple Mo & White (1996) bias formula has been shown not to correctly reproduce the correlation of low mass haloes in numerical simulations. Several alternative fits have been recently proposed (Jing 1998; Porciani, Catelan & Lacey 1999; Sheth & Tormen 1999; Jing 1999). In this paper we adopt the relations recently introduced by Sheth & Tormen (1999), which have been shown to produce an accurate fit of the distribution of the halo populations in the GIF simulations (Kauffmann et al. 1999). The new relations read

$$\bar{n}(z, M) = \sqrt{\frac{2aA^2}{\pi}} \frac{3H_0^2 \Omega_{\text{om}}}{8\pi G} \frac{\delta_c}{M D_+(z) \sigma_M} \left[1 + \left(\frac{D_+(z) \sigma_M}{\sqrt{a} \delta_c} \right)^{2p} \right] \left| \frac{d \ln \sigma_M}{d \ln M} \right| \exp \left[-\frac{a \delta_c^2}{2 D_+^2(z) \sigma_M^2} \right] \quad (16)$$

and

$$b(M, z) = 1 + \frac{1}{\delta_c} \left(\frac{a \delta_c^2}{\sigma_M^2 D_+^2(z)} - 1 \right) + \frac{2p}{\delta_c} \left(\frac{1}{1 + [\sqrt{a} \delta_c / (\sigma_M D_+(z))]^{2p}} \right). \quad (17)$$

Here σ_M^2 is the mass-variance on scale M , linearly extrapolated to the present time ($z = 0$), δ_c the critical linear overdensity for spherical collapse and $D_+(z)$ the linear growth factor of density fluctuations, normalized to unity at $z = 0$. Following Sheth & Tormen (1999), we adopt their best-fit parameters $a = 0.707$, $p = 0.3$ and $A \approx 0.3222$, while the standard (Press & Schechter and Mo & White) relations are recovered for $a = 1$, $p = 0$ and $A = 1/2$. Sheth, Mo & Tormen (1999) have shown that these expressions naturally arise when an ellipsoidal collapse model replaces the usual spherical collapse in a Press-Schechter-like approach. A possible limitation with the use of this bias formula comes from exclusion effects among dark matter haloes, which would reduce the halo correlation function below some characteristic separation, depending on the halo mass (e.g. Sheth & Lemson 1999). At first glance, one would expect this effect to take place below the Lagrangian radius of the considered haloes. On the other hand, as argued by Benson et al. (2000), haloes move somewhat from their original position, so the largest exclusion effects should be expected below the virial halo radius. In our case, this limitation would affect our estimate of the correlation function for separations $r \ll 5 h^{-1}$ Mpc.

3.2 Evolution of the mass auto-correlation function

To predict the clustering properties of X-ray clusters we need a description of the matter covariance function and its redshift evolution. To this purpose, Matarrese et al. (1997) and Moscardini et al. (1998) used an accurate method, based on Hamilton et al. (1991) original ansatz, as later developed by Peacock & Dodds (1994), Jain, Mo & White (1995) and Peacock & Dodds (1996), to evolve $\xi(r, z)$ into the fully non-linear regime. This technique allows to take into account different background cosmologies and different initial perturbation spectra, within the bottom-up hierarchical scenario for structure formation in the Universe.

We adopt here the method of Peacock & Dodds (1996), which deals with the (dimensionless) power-spectrum Δ^2 :

$$\Delta^2(k, z) = \frac{1}{2\pi^2} k^3 P(k, z), \quad (18)$$

which is related to the two-point correlation function by

$$\xi(r, z) = \int \frac{dk}{k} \Delta^2(k, z) \frac{\sin kr}{kr}. \quad (19)$$

In the linear regime, one has $\Delta_{\text{lin}}^2(k, z) = D_+^2(z) \Delta_{\text{lin}}^2(k, 0)$. According to Peacock & Dodds (1996) the non-linear power-spectrum is related to the linear one through the transformation

$$\Delta^2(k, z) = \mathcal{F}[\Delta_{\text{lin}}^2(k_0, z)], \quad k_0 = [1 + \Delta^2(k, z)]^{-1/3} k, \quad (20)$$

where k_0 and k are the linear and non-linear wavenumbers, respectively, and the specific form of the fitting function \mathcal{F} , whose detailed form is given in Peacock & Dodds (1996), depends on the growth suppression factor $g_\delta(z) \equiv (1+z)D_+(z)$. In the general case g_δ contains a dependence on the background cosmology. Carroll, Press & Turner (1992) found the approximate (but almost exact) expression

$$g_\delta(z|\Omega_m, \Omega_\Lambda) = \frac{5}{2} \Omega_m [\Omega_m^{4/7} - \Omega_\Lambda + (1 + \Omega_m/2)(1 + \Omega_\Lambda/70)]^{-1}, \quad (21)$$

with $\Omega_m = \Omega_{0m}(1+z)^3/E^2(z)$ and $\Omega_\Lambda = \Omega_{0\Lambda}/E^2(z)$.

The form of $\mathcal{F}(x)$ given by Peacock & Dodds (1996) assumes a power-law initial spectrum described by an index n . For models which are not described by pure power-law spectra, such as the Cold Dark Matter (CDM) models adopted here, one can use the same formulas, but replacing n by an effective index n_{eff} , defined by

$$n_{\text{eff}}(k_0, z) = \left. \frac{d \ln P_{\text{lin}}(k, z)}{d \ln k} \right|_{k=k_0(z)/2}. \quad (22)$$

According to Peacock & Dodds (1996) this prescription is able to reproduce the non-linear evolution with a precision of few per cent (see also the discussion in Kravtsov & Klypin 1999). The conditions under which this formalism can be applied to CDM models with $n < 1$ are discussed by Moscardini et al. (1998).

3.3 Structure formation models

In the following analysis we consider five models, all normalized to reproduce the local cluster abundance, following the Eke, Cole & Frenk (1996) analysis of the temperature distribution of X-ray clusters (Henry & Arnaud 1991). All of them belong to the general class of CDM models; their linear power-spectrum can be represented as $P_{\text{lin}}(k, 0) \propto k^n T^2(k)$, where, for the CDM transfer function $T(k)$, we use the Bardeen et al. (1986) fit. In particular, we consider

Table 1. The parameters of the cosmological models. Column 2: the present matter density parameter Ω_{0m} ; Column 3: the present cosmological constant contribution to the density $\Omega_{0\Lambda}$; Column 4: the primordial spectral index n ; Column 5: the Hubble parameter h ; Column 6: the shape parameter Γ ; Column 7: the spectrum normalization σ_8 ; Column 8: the value of the parameter η in the temperature-luminosity relation required to reproduce the observed $\log N$ - $\log S$ (see text for details).

Model	Ω_{0m}	$\Omega_{0\Lambda}$	n	h	Γ	σ_8	η
SCDM	1.0	0.0	1.0	0.50	0.45	0.52	-0.8
τ CDM	1.0	0.0	1.0	0.50	0.21	0.52	0.0
TCDM	1.0	0.0	0.8	0.50	0.41	0.52	-0.3
OCDM	0.3	0.0	1.0	0.65	0.21	0.87	-0.3
Λ CDM	0.3	0.7	1.0	0.65	0.21	0.93	-0.2

three different Einstein-de Sitter models, for which the power-spectrum amplitude corresponds to $\sigma_8 = 0.52$ (here σ_8 is the r.m.s. fluctuation amplitude in a sphere of $8h^{-1}$ Mpc). They are: a version of the standard CDM (SCDM) model with shape parameter (see its definition in Sugiyama 1995) $\Gamma = 0.45$ and spectral index $n = 1$; the so-called τ CDM model (White, Gelmini & Silk 1995), with $\Gamma = 0.21$ and $n = 1$; a tilted model (hereafter TCDM; Lucchin & Matarrese 1985), with $n = 0.8$ and $\Gamma = 0.41$, corresponding to a high (10 per cent) baryonic content (e.g. White et al. 1996; Gheller, Pantano & Moscardini 1998). We also consider an open CDM model (OCDM), with matter density parameter $\Omega_{0m} = 0.3$ and $\sigma_8 = 0.87$ and a low-density flat CDM model (Λ CDM), with $\Omega_{0m} = 0.3$, with $\sigma_8 = 0.93$ (see e.g. Liddle et al. 1996a,b and references therein). Except for SCDM, which is shown as a reference model, all these models are also consistent with the level of fluctuations observed by COBE (Bunn & White 1997); for TCDM consistency is achieved by taking into account the possible contribution of gravitational waves to large-angle CMB anisotropies (e.g. Lucchin, Matarrese & Mollerach 1992; Lidsey & Coles 1992). A summary of the parameters of the cosmological models used in this paper is given in Table 1.

3.4 From the catalogue limiting flux to the halo mass

In order to predict the abundance and clustering of X-ray clusters in a given sample we need to relate the X-ray cluster fluxes to a corresponding halo mass at each redshift. The given band flux S corresponds to an X-ray luminosity

$$L_X(z, S) = 4\pi d_L^2(z) S, \quad (23)$$

where $d_L = (1+z)r(z)$ is the luminosity distance. To convert L_X into the total luminosity L_{bol} we perform band and bolometric corrections by means of a Raymond-Smith code, where an overall ICM metallicity of 0.3 times solar is assumed (see e.g. Borgani et al. 1999). We translate the cluster bolometric luminosity into a temperature, adopting the empirical relation

$$T = \mathcal{A} L_{bol}^{\mathcal{B}} (1+z)^{-\eta}, \quad (24)$$

where the temperature is expressed in keV and L_{bol} is in units of $10^{44} h^{-2}$ erg s $^{-1}$. In the following analysis we assume $\mathcal{A} = 4.2$ and $\mathcal{B} = 1/3$; these values allow a good representation of the local data for temperatures larger than ≈ 1 keV (e.g. David et al. 1993; White, Jones & Forman 1997; Markevitch 1998). Analysing a catalogue of local compact groups, Ponman et al. (1996) showed that at lower temperatures the $T - L_{bol}$ relation has a steeper slope ($\mathcal{B} \approx 0.1$). For these reasons we prefer to fix a minimum value for the temperature at $T = 1$ keV. Moreover, even if observational data are consistent with no evolution in the $T - L_{bol}$ relation out to $z \approx 0.4$ (Mushotzky & Scharf 1997; Donahue et al. 1999), a moderate redshift evolution described by the parameter η has been introduced to reproduce the observed $\log N$ - $\log S$ relation in the range $2 \times 10^{-14} \leq S \leq 2 \times 10^{-11}$ (see below). A similar approach has been followed also by Kitayama & Suto (1997), Mathiesen & Evrard (1998) and Borgani et al. (1999).

Finally, with the standard assumption of virial isothermal gas distribution and spherical collapse, it is possible to convert the cluster temperature into the mass of the hosting dark matter halo, namely (e.g. Eke, Cole & Frenk 1996)

$$T = \frac{7.75}{\beta_{TM}} \left(\frac{M}{10^{15} h^{-1} M_{\odot}} \right)^{2/3} E^{2/3}(z) \left(\frac{\Delta_{vir}(z)}{178} \right)^{1/3}. \quad (25)$$

The quantity Δ_{vir} represents the mean density of the virialized halo in units of the critical density at that redshift (e.g. Bryan & Norman 1998 for fitting formulas). We assume $\beta_{TM} = 1.17$, which is in agreement with the results of different hydrodynamical simulations (Bryan & Norman 1998; Gheller, Pantano & Moscardini 1998; Frenk et al.

1999). Voit & Donahue (1998) discussed the validity of the previous relation in the case of small Ω_{0m} , where the assumption of a correspondence between the cluster formation redshift and that at which we are observing it is less accurate.

Once the relation between observed flux and halo mass at each redshift is established we can obtain the redshift distribution $\mathcal{N}(z)$ as

$$\mathcal{N}(z) = 4\pi g(z) \int_{\mathcal{M}} d \ln M \phi(z, M) \bar{n}(z, M), \quad (26)$$

where the selection function $\phi(z, M)$ accounts for the sample sky coverage $\Omega_{\text{sky}}(S)$, which is formally defined as the area of the sky covered by the sample as a function of the limiting flux S , i.e. $\phi(z, M) = \Omega_{\text{sky}}[S(z, M)]/4\pi$.

In Figure 1 we show the differential number counts $n(S)$ (per unit solid angle) as a function of the limiting flux S_{lim} (defined in the 0.5–2 keV band), for three different cosmological models (SCDM, OCDM and Λ CDM). The differential number counts are computed from the relation

$$n(S) = \int_0^\infty dz g(z) \bar{n}(z, M) \left. \frac{\partial \ln M}{\partial S} \right|_z, \quad (27)$$

assuming $\phi = 1$. In the same plot we report the observational data coming from the RDCS sample (Rosati et al. 1998) up to fluxes of $\simeq 5 \times 10^{-13} \text{ erg s}^{-1} \text{ cm}^{-2}$ and from the RASS1 catalogue (De Grandi et al. 1999a) for higher fluxes. The left panel shows the theoretical predictions obtained under the assumption of no evolution in the temperature-luminosity relation, i.e. with $\eta = 0$ in eq.(24). The agreement with the observational data is good but there is some tendency to overestimate the number counts at very low fluxes. The situation is improved in the right panel which shows the results obtained allowing a redshift evolution of the $T - L_{\text{bol}}$ relation to fit the data. In this case the observed $\log N - \log S$ relation is well reproduced by all cosmological models. The required best-fitting values of η for SCDM, τ CDM, TCDM, OCDM and Λ CDM are reported in Table 1. In the following analysis we will show results obtained with these values of η ; a short discussion of the effect of the alternative choice $\eta = 0$ will be presented in Section 5.1.

We note that the SCDM model predicts more clusters than low-density models. This might appear counter-intuitive. In fact the cosmological models are normalized using the local cluster abundance which declines, when the matter density is high, more rapidly with increasing redshift. This effect (shown also in the following redshift distributions) is due to the larger number of low-temperature clusters (we assume a minimum temperature of 1 keV) predicted by the SCDM model. We remind that the cluster abundance normalisation results from the analysis of objects with a typical temperature of about 5-6 keV. The use of a different normalization can help in sorting this problem out. The point is discussed in Section 5.2, where we show how our results change if σ_8 is desumed from the X-ray luminosity function which extends to clusters with temperature down to ~ 1 keV.

4 THEORETICAL PREDICTIONS FOR VARIOUS CATALOGUES

4.1 Description of the catalogues

In the following analysis we will apply our method to four different cases. The first three applications refer to presently existing data: the ROSAT Brightest Cluster Sample (BCS); the X-ray brightest Abell-type cluster sample (XBACs); the ROSAT-ESO Flux Limited X-ray sample (REFLEX). The fourth and last case will be an example of possible future space missions: for that we will consider a survey with characteristics similar to those which were expected from the unfortunate satellite ABRIXAS. Here we will give the relevant information about these surveys. We refer to the original papers for more details.

- The BCS catalogue (Ebeling et al. 1997, 1998; Crawford et al. 1999) is an X-ray selected, flux-limited sample of 201 galaxy clusters with $z \leq 0.3$ drawn from the ROSAT All-Sky Survey in the northern hemisphere ($\delta \geq 0^\circ$) and at high Galactic latitudes ($|b_{ll}| \geq 20^\circ$). The limiting flux is $S_{\text{lim}} = 4.45 \times 10^{-12} \text{ erg cm}^{-2} \text{ s}^{-1}$ in the 0.1–2.4 keV band. Since its sky-coverage $\Omega_{\text{sky}}(S)$ is not available, we use $\Omega_{\text{sky}}(S) = \text{const} \simeq 4.13$ steradians for fluxes larger than S_{lim} .

- The XBACs catalogue (Ebeling et al. 1996) is an all-sky X-ray sample of 242 Abell galaxy clusters extracted from the ROSAT All-Sky Survey data. Being optically selected, it is not a complete flux-limited catalogue. The sample covers high Galactic latitudes ($|b_{ll}| \geq 20^\circ$). The adopted limiting flux is $S_{\text{lim}} = 5 \times 10^{-12} \text{ erg cm}^{-2} \text{ s}^{-1}$ in the 0.1–2.4 keV band. Also in this case, since the actual sky coverage is not published, we will adopt $\Omega_{\text{sky}}(S) = \text{const} \simeq 8.27$ steradians for fluxes larger than S_{lim} . Due to the aforementioned selection effects, the XBACs luminosity function $N(L)$ in the faint part is much lower than that obtained from other catalogues (e.g. Ebeling et al. 1997; Rosati et al. 1998; De Grandi et al. 1999b). Using a redshift evolution of the temperature-luminosity relation, we forced our models to be consistent with the number counts. For this reason we have to introduce in the models for XBACs

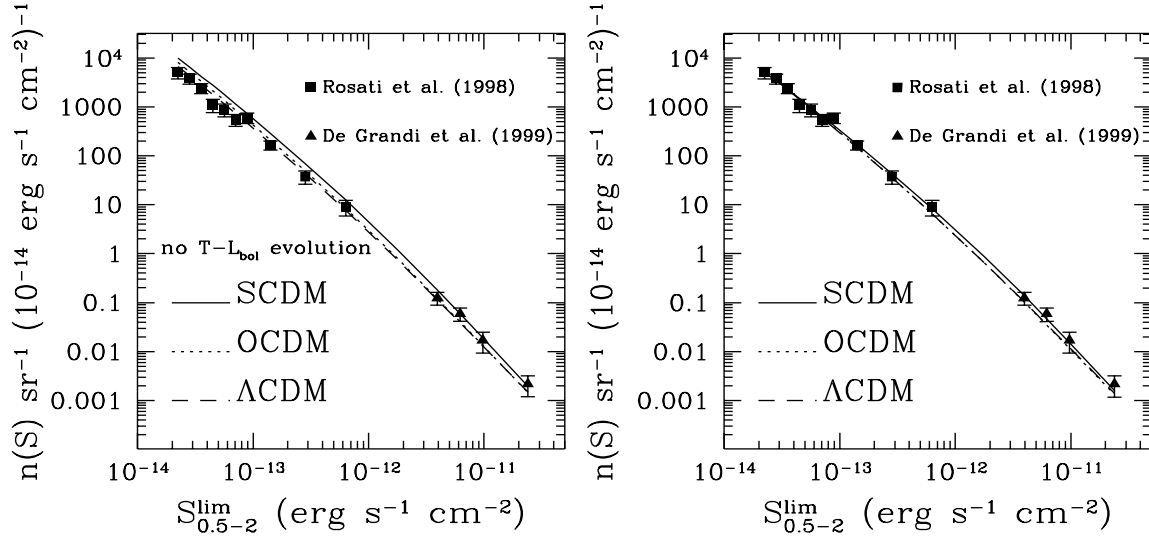


Figure 1. The differential number counts (per unit solid angle) $n(S)$ as a function of the limiting flux S_{lim} computed in the 0.5–2 keV band. The observational results (with 1- σ errorbars) obtained by Rosati et al. (1998) and De Grandi et al. (1999a) are shown by filled squares and filled triangles, respectively. Different lines refer to theoretical predictions for various cosmological models: SCDM (solid lines), OCDM (dotted lines) and LCDM (dashed lines). The left panel shows the results obtained with no evolution in the temperature-luminosity relation [i.e. $\eta = 0$ in eq.(24)]; the right panel presents the results for the models adopting the value of η which best-fits the observational data (see text for more details).

its incompleteness $I(L)$, defined as the ratio between its luminosity function $N_{\text{XBACs}}(L)$ and $N_{\text{best}}(L)$, which is a combination of the results for RDCS at low L (Rosati et al. 1998) and for BCS at high L (Ebeling et al. 1997):

$$I(L) = N_{\text{XBACs}}(L)/N_{\text{best}}(L). \quad (28)$$

The adopted parameters for the luminosity function, usually fitted as $N(L) = KL^{-\alpha} \exp(L/L^*)$, are $K = 2.8$, $\alpha = 1.1$, $L^* = 5.5$ for N_{XBACs} and $K = 3.26$, $\alpha = 1.83$, $L^* = 5.5$ for N_{best} ; in the previous formula L^* is in units of $10^{44} \text{ erg s}^{-1}$ in the band 0.5–2 keV (with $h = 0.5$) and K is in units of $10^{-7} \text{ Mpc}^{-3} L^{\alpha-1}$. The clustering properties of this catalogue have been studied by different authors (Abadi, Lambas & Muriel 1998; Borgani, Plionis & Kolokotronis 1999) giving a correlation length in the range $20 \lesssim r_0 \lesssim 26 h^{-1} \text{ Mpc}$.

- The REFLEX survey (Böhlinger et al. 1998; Guzzo et al. 1999) is a large sample of optically confirmed X-ray clusters selected from the ROSAT All-Sky Survey. The sample, nearly completed, will contain about 700 clusters in the southern hemisphere, at high Galactic latitude ($|b_{\text{II}}| \geq 20^\circ$). For our computations, we use the actual sky coverage kindly provided by H. Böhlinger and C. Collins and defined in the ROSAT band (0.1–2.4 keV). In order to make predictions for the cluster sample analysed by Collins et al. (2000), which contains approximately 450 objects, we adopt the sky coverage only above a minimum flux of $S_{\text{lim}} = 3 \times 10^{-12} \text{ erg cm}^{-2} \text{ s}^{-1}$, where it falls to 97.3 per cent of the whole surveyed region (4.24 steradians). The clustering properties of a part of this catalogue, known as RASS1 Bright Sample (De Grandi et al. 1999a) and containing 130 galaxy clusters with flux larger than $S_{\text{lim}} = 3 \times 10^{-12} \text{ erg cm}^{-2} \text{ s}^{-1}$ in the ROSAT soft band 0.5–2 keV, have been analysed by Moscardini et al. (2000) and compared with the predictions of different cosmological models obtained with the same technique presented here.

- The ABRIXAS satellite (Trümper, Hasinger & Staubert 1998) has been unluckily lost at the end of April 1999 because of problems with energy supply. We use here the characteristics of the survey of X-ray selected clusters which was expected to be obtained from its observations as an example of an application of our method to possible future samples of X-ray galaxy clusters. In the plans, the ABRIXAS catalogue would have covered the area at high Galactic latitudes ($|b_{\text{II}}| \geq 20^\circ$) up to a limiting flux of $S_{\text{lim}} = 5 \times 10^{-13} \text{ erg cm}^{-2} \text{ s}^{-1}$ in the 0.5–2 keV band. We will assume a constant sky coverage $\Omega_{\text{sky}}(S) \simeq 8.27$ steradians for fluxes larger than S_{lim} .

4.2 Physical properties of the clusters in different catalogues

In this subsection we discuss the redshift dependence of the physical properties of the clusters contained in the catalogues presented in the previous subsection. These results are obtained using the relations described in Section

3.4 and linking the limiting flux to the X-ray luminosity, the luminosity to the temperature and finally the temperature to the mass of the hosting dark matter halo.

In the upper panels of Figure 2 we present the behaviour (as a function of the redshift z) of the minimum temperature T_{\min} corresponding to the limiting flux of the various catalogues. The results are here presented only for three cosmological models (SCDM, OCDM, Λ CDM). The minimum temperature is a strongly increasing function of both the redshift and the limiting flux, while the dependence on the cosmological model is not so evident. For example, clusters with a temperature as high as 10 keV can enter the catalogues only up to $z \simeq 0.2$ when the limiting flux of BCS and XBACs is considered, $z \simeq 0.3 - 0.35$ for the REFLEX limits, and $z \simeq 0.4 - 0.5$ for the ABRIXAS ones.

In the lower panels of Figure 2 we show the redshift dependence of the minimum mass M_{\min} . Once again the result is strongly dependent on S_{lim} . As a consequence, the different samples can contain clusters with quite different ranges of masses: given a redshift, the BCS and XBACs catalogues (which have very similar limits, therefore leading to very similar minimum temperatures and masses) tend to have richer (more massive) clusters than the ABRIXAS and REFLEX ones. Note that Suto et al. (2000) found that M_{\min} corresponding to a given value of the limiting flux S_{lim} decreases for $z \gtrsim 1$. This effect is expected due to the redshift dependences in eqs.(23-25). Our different choices for \mathcal{B} and η in eq.(24) shift the turn-around of M_{\min} to much larger redshifts, not relevant for this study.

In order to predict the clustering properties, in our model one needs to know the expected redshift distribution $\mathcal{N}(z)$ for the given catalogue. The results, computed by using eq.(26), are shown in Figure 3 for SCDM, OCDM and Λ CDM models. Of course, the number of clusters increases with decreasing limiting flux. In this case the differences between BCS and XBACs, which have similar S_{lim} , are due to the different sky coverage and to the function $I(L)$ introduced to correct for the XBACs' incompleteness. As expected, the redshift distribution for the Einstein-de Sitter model is less extended towards high redshifts than in the models with low matter density parameter, due to the freezing of the perturbation growth in the latter case.

The last ingredient of our model is the redshift evolution of the effective bias $b_{\text{eff}}(z)$, computed from eq.(12). In Figure 4 we show the values of $b_{\text{eff}}(z)$ for the different catalogues. The effective bias is found to be an increasing function of redshift: high-redshift clusters, if existing, have a very high bias.

4.3 Clustering predictions

We start by applying our method to the XBACs catalogue, because in this case we can compare directly our predictions to the observational clustering properties obtained by two different groups. Abadi, Lambas & Muriel (1998) found that the XBACs spatial correlation function can be fitted by the usual power-law relation $\xi(r) = (r/r_0)^{-\gamma}$ with $\gamma = 1.92$ and $r_0 = 21.1_{-2.3}^{+1.6} h^{-1}$ Mpc (errorbars correspond to 1σ). Borgani, Plionis & Kolokotronis (1999), who adopted an analytical approximation to the bootstrap errors for the variance of $\xi(r)$, found $\gamma = 1.98_{-0.53}^{+0.35}$ and a slightly larger value of $r_0 = 26.0_{-4.7}^{+4.1} h^{-1}$ Mpc (errorbars in this case are $2\text{-}\sigma$ uncertainties). Figure 5 compares these observational estimates (shown by the shaded regions) to the theoretical predictions of the cosmological models here considered: the three $\Omega_{\text{om}} = 1$ models (SCDM, τ CDM and TCDM) are presented in the left panel while the two $\Omega_{\text{om}} = 0.3$ models (OCDM and Λ CDM) are in the right one. In the plot 'mock-observational' errorbars are reported only for SCDM and OCDM models, for clarity: these are obtained by bootstrap resampling the number of expected pairs in each separation bin (Mo, Jing & Börner 1992). We find that all Einstein-de Sitter models display too small correlations. Their correlation lengths are smaller than the observational results: we find $r_0 \simeq 11, 15, 13 h^{-1}$ Mpc for SCDM, TCDM and τ CDM, respectively. On the contrary, both the OCDM and Λ CDM models give very similar results and are in better agreement with the observational data ($r_0 \simeq 20 - 22 h^{-1}$ Mpc). Similar conclusions have been reached by Moscardini et al. (2000) from the analysis of the RASS1 Bright Sample.

The theoretical predictions for the other catalogues here considered (BCS, REFLEX and ABRIXAS) are shown in Figure 6. Our results show that the amplitude of the spatial correlation function is an increasing function of the limiting flux. This is in agreement with what found by Moscardini et al. (2000), using the RASS1 Bright Sample data alone, and by Suto et al. (2000) in a more general analysis of flux-limited surveys made with a technique similar to that applied here. Moreover, we find that the two non-Einstein-de Sitter models with $\Omega_{\text{om}} = 0.3$ display similar clustering properties and tend to have larger amplitudes than the $\Omega_{\text{om}} = 1$ models. Note that preliminary analyses of the two-point spatial correlation and of the power-spectrum of the REFLEX sample (Collins et al. 2000; Guzzo et al. 1999; Schuecker et al. 2000), lead to a correlation length $r_0 \simeq 18 h^{-1}$ Mpc. If this result will be confirmed, the comparison with our theoretical predictions will give further support to cosmological models with a low matter density parameter.

From the previous analysis we found that the amplitude of $\xi(r)$ decreases by lowering the limiting flux. This result can be related to the study of the richness dependence of the cluster correlation function. In fact, when we change the observational limits, the resulting sample can have a different mean intercluster separation d_c . A recent

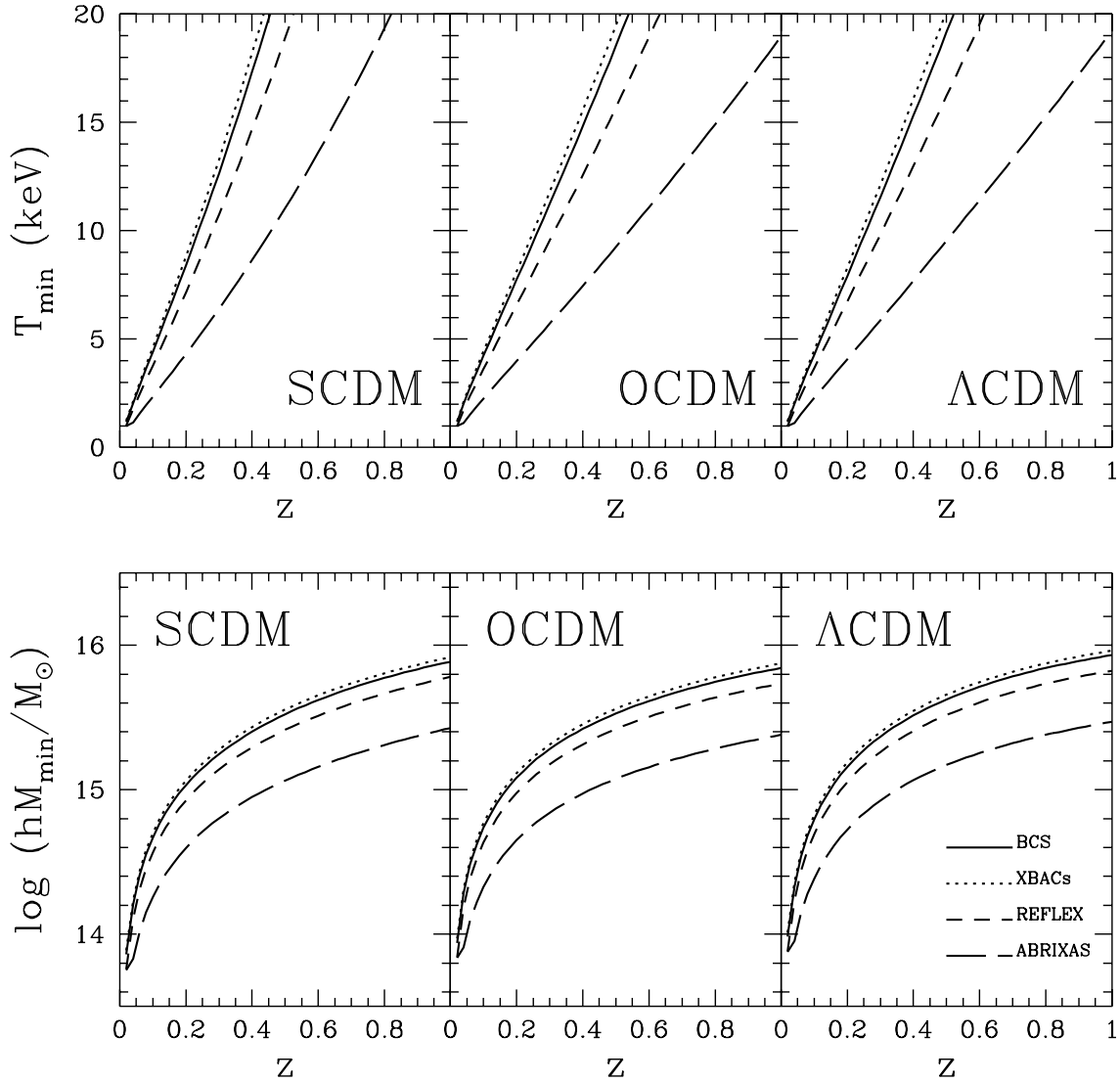


Figure 2. The behaviour of the minimum temperature T_{\min} (upper panels) and of the minimum mass M_{\min} (lower panels) for the clusters included in the flux-limited samples as a function of the redshift z . Different lines refer to results for different catalogues: BCS (solid line), XBACs (dotted line), REFLEX (short dashed) and ABRIXAS (long dashed). Predictions for different cosmological models are shown in the different columns: SCDM (left), OCDM (centre) and Λ CDM (right).

analysis of the APM clusters made by Croft et al. (1997) found a $r_0 - d_c$ dependence which is milder than the linear relation obtained by Bahcall & West (1992) for the Abell clusters. In order to give a more quantitative estimate of this dependence, we use our model to predict the value of the correlation length r_0 in catalogues where we vary the limiting X-ray flux S_{lim} (defined in the energy band 0.5–2 keV). The results, displayed in Figure 7, confirm that for all the cosmological models the correlation length r_0 grows with S_{lim} . By changing the limiting flux by four orders of magnitude (from $S_{\text{lim}} = 10^{-14}$ to $S_{\text{lim}} = 10^{-10}$ erg s $^{-1}$ cm $^{-2}$), the correlation length varies by a factor of $\simeq 2$ (from $r_0 \simeq 7 - 10$ to $r_0 \simeq 15 - 20h^{-1}$ Mpc for the Einstein-de Sitter models and from $r_0 \simeq 12$ to $r_0 \simeq 25h^{-1}$ Mpc for the $\Omega_{\text{om}} = 0.3$ models).

A similar analysis has been made by Suto et al. (2000, see their Figure 8). Even if the results cannot be directly compared because they adopt cosmological models with different values of the parameters (Ω_{om} , Γ and σ_8), a different (but almost equivalent) formalism for the past-light cone effect and different bias prescriptions, temperature-luminosity and mass-temperature relations, it is possible to notice that there is general qualitative agreement. However, our model tends to predict smaller correlation lengths (by approximately 30 per cent). As we

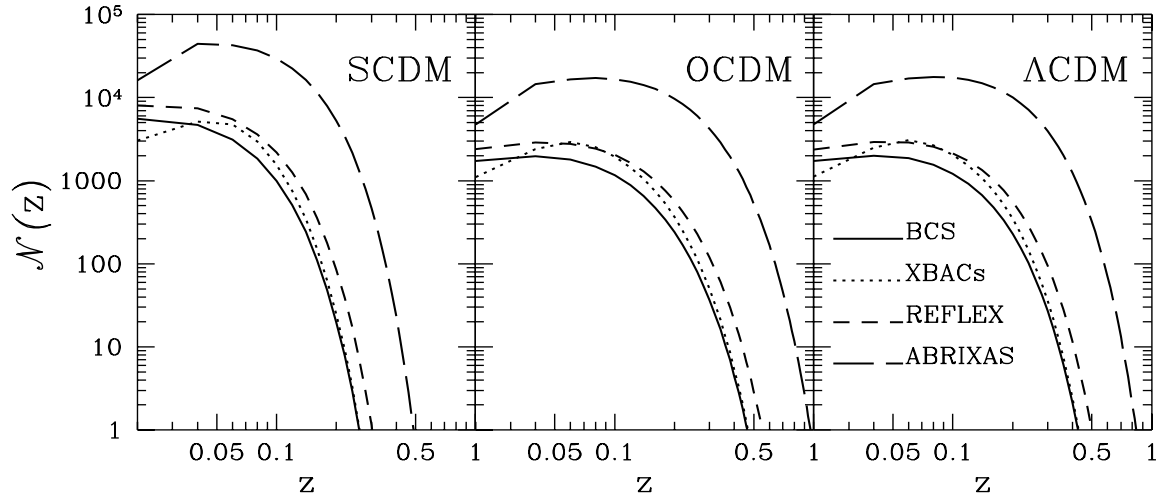


Figure 3. The redshift distribution $\mathcal{N}(z)$ for the clusters included in the flux-limited samples. Different lines refer to results for different catalogues: BCS (solid line), XBACs (dotted line), REFLEX (short dashed) and ABRIXAS (long dashed). Different panels show the predictions for various cosmological models: SCDM (left), OCDM (centre) and Λ CDM (right).

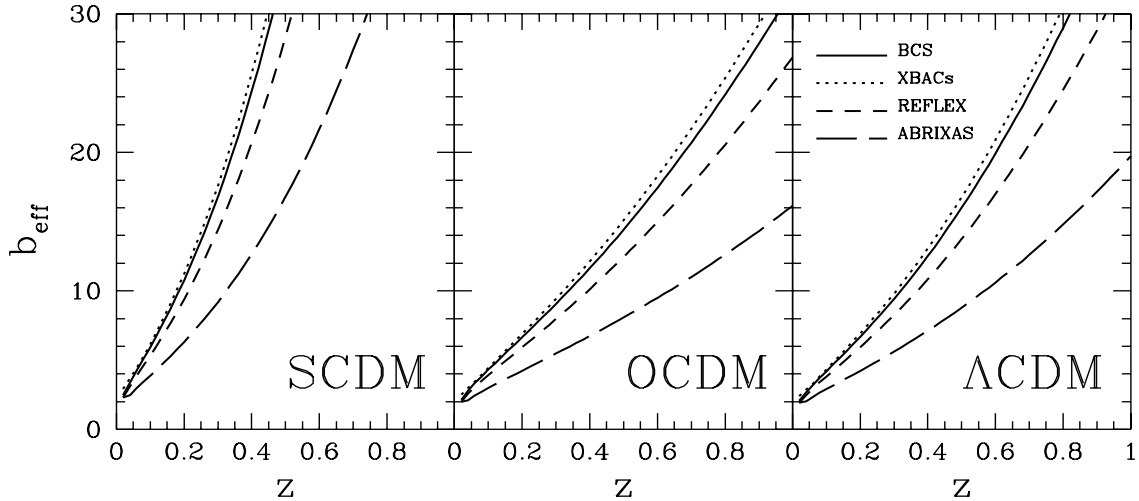


Figure 4. The behaviour of the effective bias b_{eff} for the clusters included in the flux-limited samples as a function of the redshift z . Different lines refer to results for different catalogues: BCS (solid line), XBACs (dotted line), REFLEX (short dashed) and ABRIXAS (long dashed). Different panels show the predictions for various cosmological models: SCDM (left), OCDM (centre) and Λ CDM (right).

will discuss in Section 5.1, part of this difference comes from the values of \mathcal{B} used in the temperature-luminosity relation [see eq.(24)]: $\mathcal{B} = 1/3.4$ and $1/3$ in Suto et al. (2000) and in this paper, respectively. Moreover, in their approach Suto et al. include a method to account for redshift-space distortion effects (here not considered) which tends to increase the correlation estimates (see the discussion at the end of Section 2.1).

The dependence of the correlation length on the survey flux limit can be used to give a partial explanation of the difference between the early results derived by Romer et al. (1994) and those obtained in more recent analyses (Abadi, Lambas & Muriel 1998; Borgani, Plionis & Kolokotronis 1999; Moscardini et al. 2000). In fact the Romer et al.' catalogue is deeper ($S_{\text{lim}} \simeq 10^{-12}$ erg s $^{-1}$ cm $^{-2}$ in the 0.1 – 2.4 keV band) than both XBACs and the RASS1

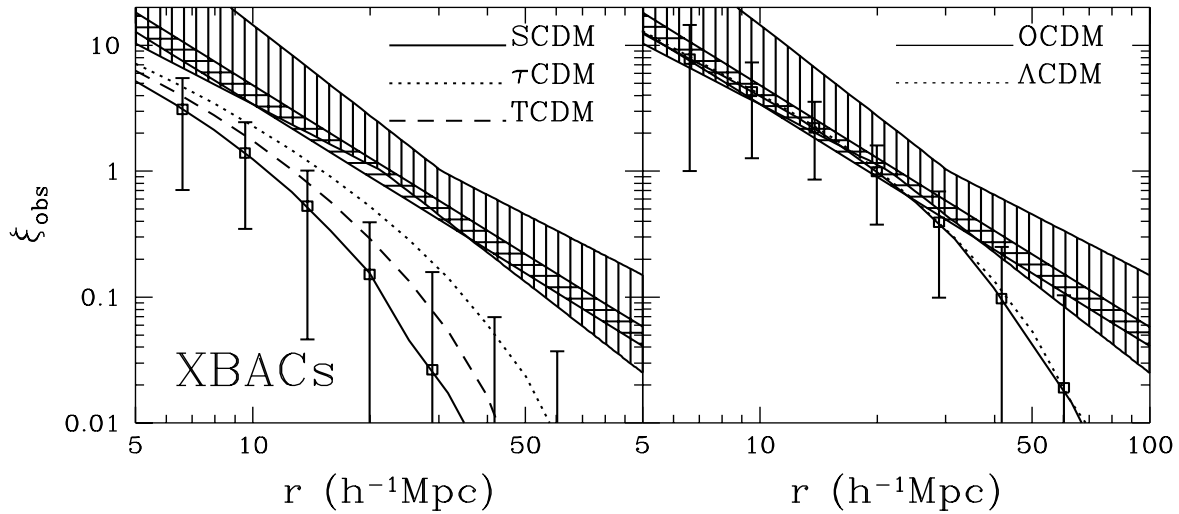


Figure 5. Comparison of the observed spatial correlation for clusters in the XBACs sample with the predictions of the various cosmological models. The observational results are shown by the shaded areas: the horizontal shaded region refers to the $(1-\sigma)$ estimates obtained by Abadi, Lambas & Muriel (1998), the vertical shaded one shows the $(2-\sigma)$ estimates by Borgani, Plionis & Kolokotronis (1999). In the left panel we present the SCDM model (solid line), the τ CDM model (dotted line) and the TCDM model (short-dashed line); in the right panel we show the OCDM model (solid line) and the Λ CDM model (dotted line). Bootstrap estimates of the errorbars ($1-\sigma$) for the theoretical predictions are shown only for the SCDM and OCDM models for clarity.

Bright Sample. However, we have also to remind that the results of Romer et al. (1994) can be affected both by the absence of a study of the sample sky coverage and by incompleteness effects. In fact the cluster catalogue was derived drawing on X-ray information from the ROSAT standard analysis software (SASS), which was not optimized for the analysis of extended sources, as shown by De Grandi et al. (1997).

By using a survey as deep and extended as that which was planned with the ABRIXAS satellite, it would be possible to address the problem of the redshift evolution of the spatial correlation function $\xi(r)$. In Figure 8 we show the theoretical predictions for $\xi(r)$ obtained if the ABRIXAS catalogue is divided in two subsamples, $z < 0.2$ and $z > 0.2$. All cosmological models display a larger amplitude at higher redshifts. The difference between the $z < 0.2$ and $z > 0.2$ subsamples is significant: the correlation length moves from $r_0 \simeq 8$ to $r_0 \simeq 15h^{-1}$ Mpc for the SCDM model and $r_0 \simeq 15$ to $r_0 \simeq 25h^{-1}$ Mpc for the OCDM and Λ CDM models. Notice that the errorbars for the high-redshift subsample in the SCDM model are not shown because they are very large due to the small number of expected objects.

The power-spectrum analysis is an alternative way to study the clustering properties of a given catalogue. However, up to now this technique has been very seldom applied to X-ray selected clusters because of the difficulties to correctly take into account the actual sky coverage (see however Schuecker et al. 2000). By using our formalism [see eq.(14)] we can obtain the expected power-spectrum $P_{\text{obs}}(k)$ measured by the different surveys. The results for SCDM, OCDM and Λ CDM are shown in Figure 9. As it is possible to notice, given a cosmological model, the shape of $P_{\text{obs}}(k)$ does not change by varying the limiting flux: the unique effect is the change of the amplitude which decreases when S_{lim} decreases.

To conclude this subsection we would like to stress the relevance of light-cone effects in the present problem. Several authors have estimated the spatial clustering of X-ray clusters in flux-limited surveys using either analytical treatments or N-body simulations at a fixed redshift (typically chosen to coincide with the median redshift of the catalogue). The level of inaccuracy inherent in such an approach, even for shallow surveys, has been already discussed in (Moscardini et al. 2000), who found that for the RASS1 Bright sample the traditional method would lead to a 20 per cent overestimate of the correlation length. For deeper surveys, such as ABRIXAS, we find that the error would be even larger, reaching approximately 25 per cent in the case of the cosmological models with $\Omega_{0m} = 0.3$. A somewhat better approximation would be obtained by considering constant-time simulations (or analytical expressions for the two-point function) at an “effective redshift” z_{eff} , defined as the peak of $\mathcal{N}^2(z)/g(z)$ of the sample [see eq.(8)].

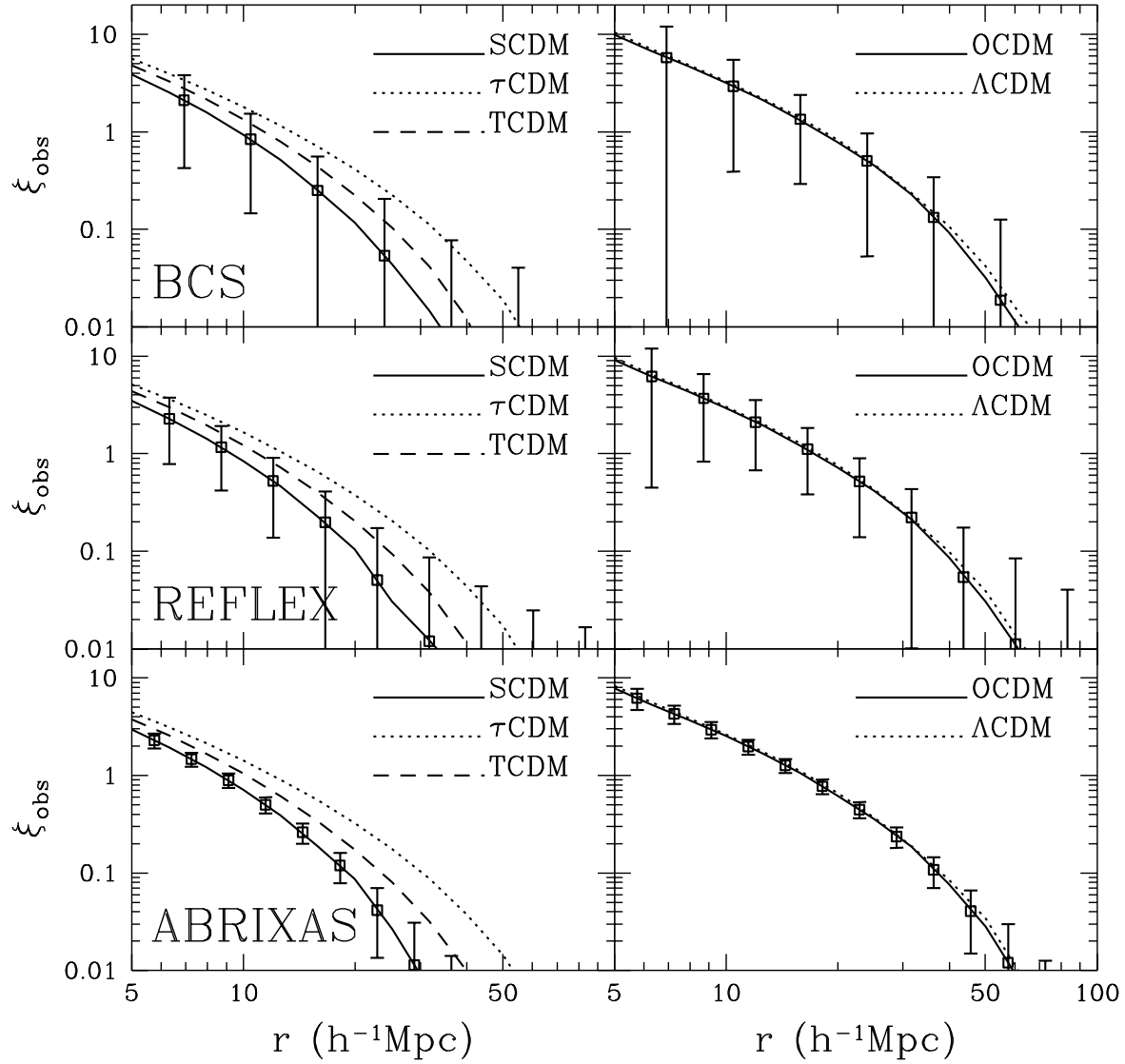


Figure 6. Predictions for the spatial correlation of X-ray selected clusters in the different samples. Results refer to the BCS sample (upper row), the REFLEX sample (central row) and the ABRIXAS sample (lower row). Different cosmological models are considered. In the left column we present the SCDM model (solid line), the τ CDM model (dotted line) and the TCDM model (short-dashed line); in the right column we show the OCDM model (solid line) and the Λ CDM model (dotted line). Bootstrap estimates of the errorbars ($1-\sigma$) for the theoretical predictions are shown only for the SCDM and OCDM models for clarity.

4.4 Strategy for future surveys

Another possible application of our technique is in the preparation of the strategy for future surveys. A typical problem to be addressed is the choice of the limiting flux to be reached (related to a minimum number of counts) and of the size of the sky area \mathcal{A} to be covered. Of course, the best solution would be to have small S_{lim} and large \mathcal{A} , but, given a finite life-time for an X-ray satellite, the two choices are in competition. To discuss this problem, we will consider two different surveys with characteristics already possible with the presently proposed space missions (see e.g. Chincarini 1999). The first one is meant to represent an example of a survey covering a wide area but with a fainter limiting flux (hereafter called ‘WIDE’); the second one (hereafter ‘DEEP’) simulates a very deep survey but with a more limited sky coverage. We choose as characteristic parameters $S_{\text{lim}} = 3 \times 10^{-14}$ erg cm $^{-2}$ s $^{-1}$ and $\mathcal{A} = 1000$ deg 2 to define the WIDE catalogue, and $S_{\text{lim}} = 7 \times 10^{-15}$ erg cm $^{-2}$ s $^{-1}$ and $\mathcal{A} = 100$ deg 2 for the DEEP one (the fluxes are in the 0.5–2 keV band). The predictions for both the spatial and angular correlation functions

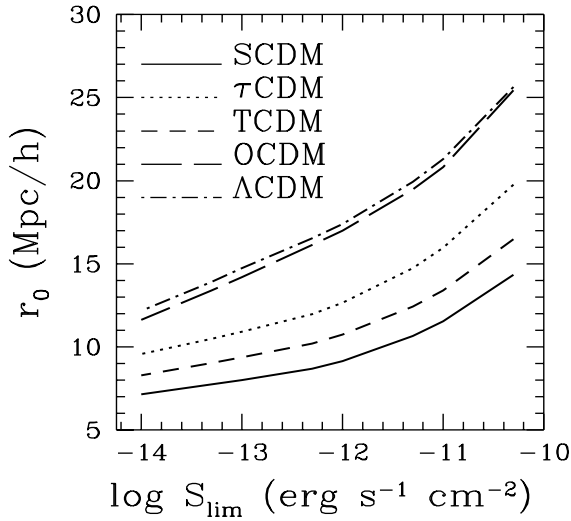


Figure 7. The behaviour of the correlation length r_0 as a function of the limiting X-ray flux S_{lim} . The predictions of the various theoretical models are shown: SCDM model (solid line), τ CDM model (dotted line), TCDM model (short-dashed line), OCDM model (long-dashed line) and Λ CDM model (dotted-dashed line).

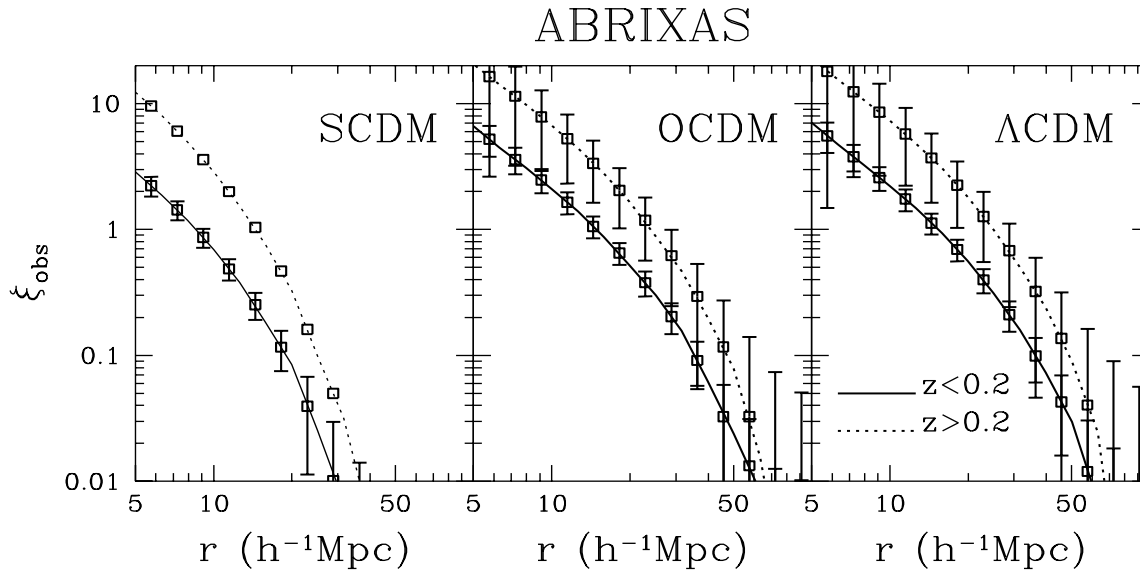


Figure 8. Predictions for the redshift evolution of the spatial correlation $\xi(r)$ of X-ray selected clusters. Results refer to two subsamples of the ABRIXAS catalogue: $z < 0.2$ (solid line) and $z > 0.2$ (dotted line). Different cosmological models have been considered: SCDM (left panel), OCDM (central panel) and Λ CDM (right panel). Errorbars are 1- σ bootstrap estimates: they are not shown for the $z > 0.2$ subsample in the SCDM model, because they are very large due to the small number of predicted objects.

[computed by using eq.(15)] are shown in Figure 10. They refer only to the OCDM model, used as a working example. The important feature of this plot is the size of the errorbars which are 1- σ bootstrap estimates. For the WIDE survey the clustering signal is larger than the errorbars and can be detected also for scales larger than 2000 arcsec and $30 h^{-1}$ Mpc, for ω_{obs} and ξ_{obs} respectively. On the contrary, for the DEEP survey the angular correlation has a significant signal only up to $\simeq 500$ arcsec while the spatial correlation is completely dominated by the noise on all scales. From these results we can conclude that the best strategy to study the clustering properties should be based on wide angle, relatively shallow, surveys.

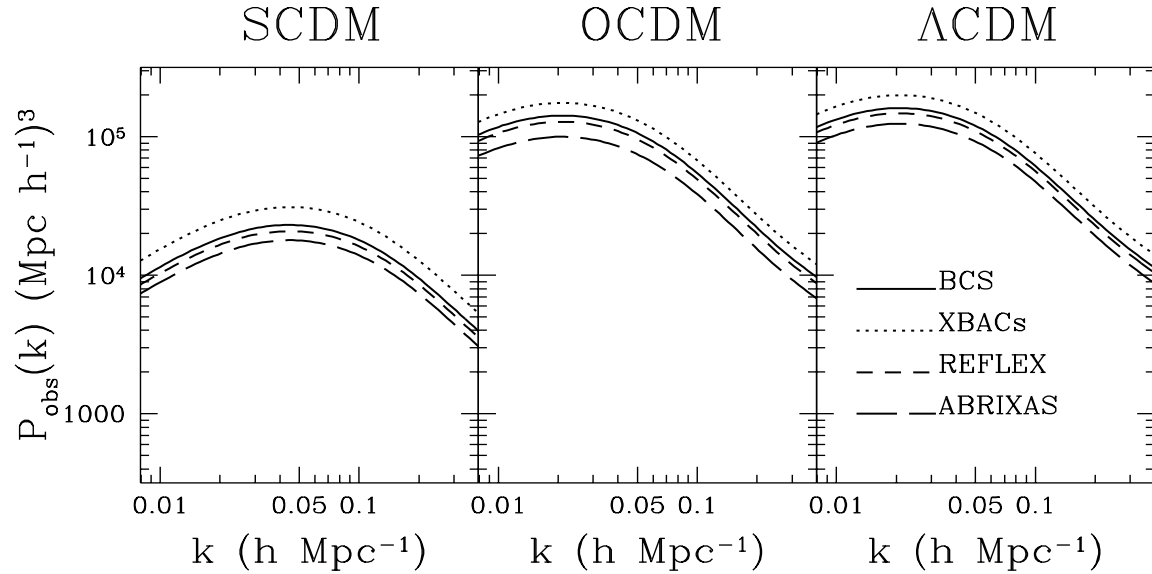


Figure 9. The theoretical predictions for the power-spectrum as measured in various catalogues: BCS (solid line), XBACs (dotted line), REFLEX (short dashed) and ABRIXAS (long dashed). Different panels show the predictions for various cosmological models: SCDM model (left), OCDM model (centre) and Λ CDM model (right).

5 ROBUSTNESS OF THE RESULTS

5.1 Dependence on the temperature-luminosity relation

Our model to predict the clustering properties of X-ray selected galaxy clusters makes use of various relations to translate the limiting flux (which is the observational quantity) into the minimum mass of the hosting dark matter halo (which is the variable preferred in the theory). The largest uncertainties inherent in this approach are in the temperature-luminosity relation. As mentioned in Section 3.4, to this aim we assumed the semi-empirical power-law relation $T \propto L_{\text{bol}}^{\mathcal{B}}$, with $\mathcal{B} = 1/3$. Moreover, we fixed a minimum temperature of 1 keV and we allowed a mild redshift evolution of the $T - L_{\text{bol}}$ relation to reproduce the cluster number counts. In this subsection we will briefly discuss the stability of the previous results with respect to changes in these choices. For that we will consider only results for the ABRIXAS survey since it is the deepest one and consequently the possible effects will be enhanced.

As already said, the value of \mathcal{B} we used is in agreement with various local (i.e. at $z \simeq 0$) estimates (e.g. David et al. 1993; White, Jones & Forman 1997; Markevitch 1998). However, different values of \mathcal{B} could be considered. The scaling relations, for example, suggest $\mathcal{B} = 1/2$; hydrodynamical simulations without inclusion of heating and cooling effects give support to this value, while smaller values of \mathcal{B} , more similar to the observational estimates, are obtained when the supernova feedback is included (e.g. Navarro, Frenk & White 1995; Cavaliere, Menci & Tozzi 1999). One more systematic effect can be due to the presence of cooling flows in the central part of the clusters. Corrections for this effect have been tried resulting in an increase of the observed \mathcal{B} (e.g. White, Jones & Forman 1997; Allen & Fabian 1998; Arnaud & Evrard 1999), in better agreement with the scaling relation.

To study the effect of this uncertainty we allow the parameter \mathcal{B} to change in the range $1/3.5 \leq \mathcal{B} \leq 1/2.5$. The results are shown in Figure 11 for SCDM, OCDM and Λ CDM. Notice that we are still imposing a minimum temperature of 1 keV and requiring a redshift evolution of the $T - L_{\text{bol}}$ relation to reproduce the counts: the resulting values of the η parameter [see eq.(24)] become larger (smaller) when the value of \mathcal{B} is decreased (increased). From the plot it is possible to see that by varying the \mathcal{B} parameter the resulting spatial correlation function does not change its shape, but only the amplitude: the larger is \mathcal{B} , the smaller is $\xi(r)$. However, the changes are quite small and with a size similar to the expected bootstrap errorbars (see e.g. Figure 6).

We also considered the effect of including clusters with temperature $T < 1$ keV (excluded in the previous analyses) adopting, only at small T , the $T - L_{\text{bol}}$ relation obtained by Ponman et al. (1996) from an analysis of groups of galaxies. This corresponds to a small value of the slope ($\mathcal{B} = 1/8.2$). The resulting change in the estimates of the spatial correlation function (not shown in the plot) are negligible and always smaller than those previously obtained. A similar result is also obtained in two other cases: when we remove the constraint on the minimum temperature and when we avoid the redshift evolution of the $T - L_{\text{bol}}$ relation (i.e. when $\eta = 0$).

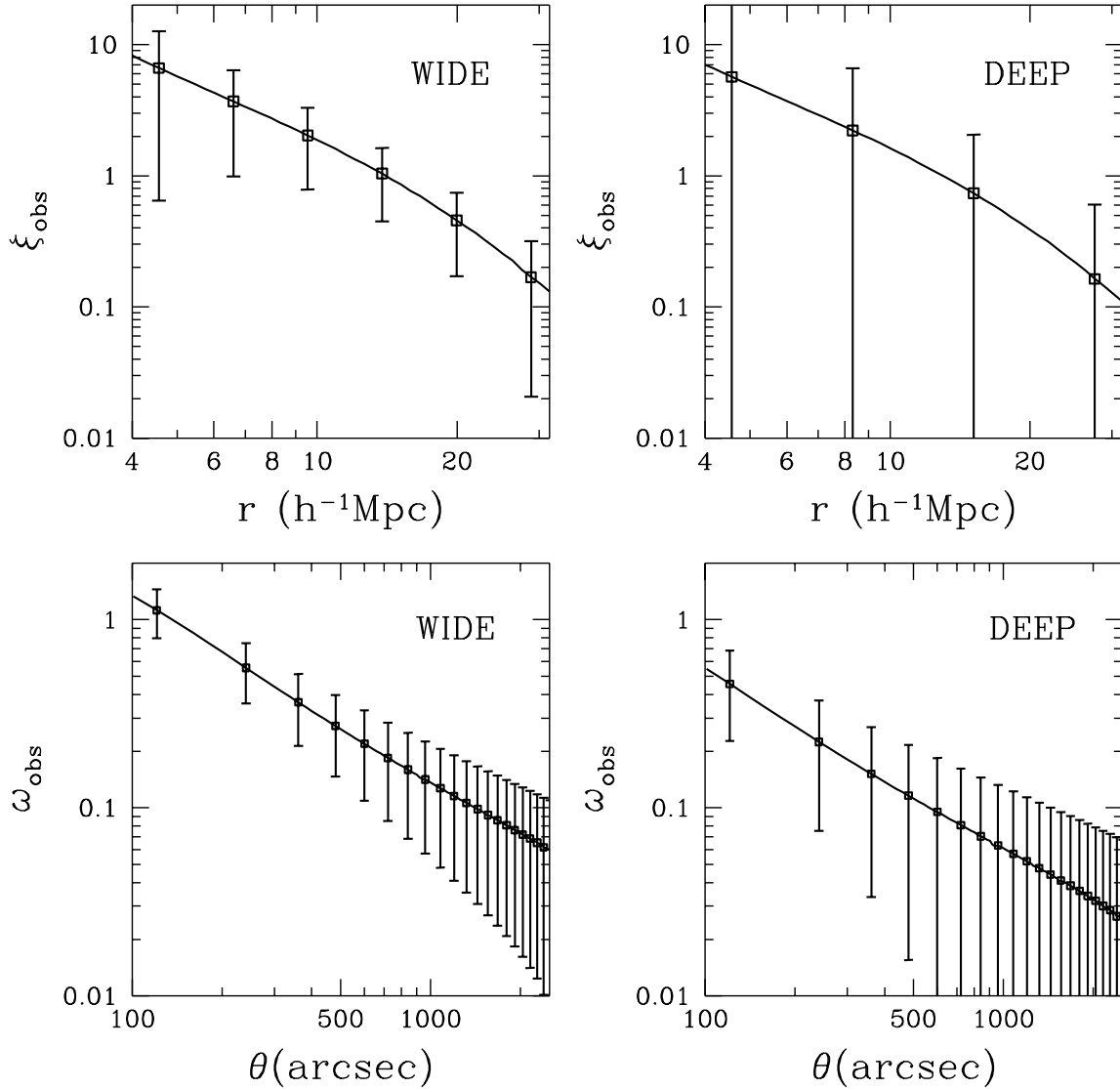


Figure 10. Theoretical predictions for the spatial correlation function ξ_{obs} (upper panels) and for the angular correlation function ω_{obs} (lower panels) for the WIDE ($S_{\text{lim}} = 3 \times 10^{-14}$ erg cm $^{-2}$ s $^{-1}$ and $\mathcal{A} = 1000$ deg 2) and DEEP ($S_{\text{lim}} = 7 \times 10^{-15}$ erg cm $^{-2}$ s $^{-1}$ and $\mathcal{A} = 100$ deg 2) surveys, shown in the left and right columns, respectively. Results are obtained using the Λ CDM model. Errorbars are 1- σ bootstrap estimates.

5.2 Dependence on the normalization of the cosmological models

In this paper we normalized the cosmological models here considered by using the local cluster abundance. In particular we adopted the values of σ_8 coming from the Eke, Cole & Frenk (1996) analysis of the temperature distribution of X-ray clusters. Strictly speaking, this approach would be appropriate only for clusters having a typical temperature of $T \sim 5 - 6$ keV, while in our analysis we consider clusters down to the imposed cutoff of $T = 1$ keV. One of the consequences of our choice is that the number of clusters predicted for SCDM is larger than that expected for the low-density models (see our Figure 3 and Figure 5 of Suto et al. 2000). Since the cosmological models are all normalized to the local cluster abundance and this abundance declines more rapidly with increasing redshift when Ω_0 is high, one would expect the opposite trend. The explanation is that SCDM has a larger number of relatively low temperature ($T \sim 1$ keV) clusters with respect to the other models because of its steeper mass (and temperature) function. This feature could introduce a dependence of some results on the imposed lower temperature.

A way to overcome the problem could be to normalize the cosmological models by using the local X-ray luminosity function. In fact, unlike the temperature function, it extends to clusters with $T \sim 1$ keV. Borgani et al. (1999) followed

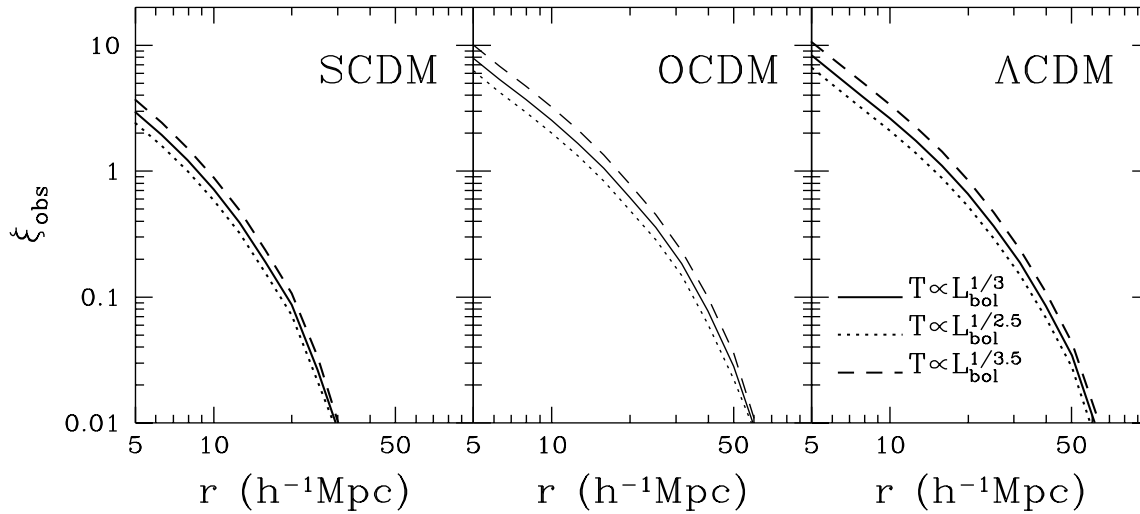


Figure 11. Theoretical predictions for the spatial correlation function ξ_{obs} estimated assuming different temperature-luminosity relations $T \propto L_{\text{bol}}^{\mathcal{B}}$: solid, dotted and dashed lines refer to $\mathcal{B} = 1/3, 1/2.5$ and $1/3.5$, respectively. Results refer to the ABRIXAS catalogue and are obtained for the SCDM model (left panel), the OCDM model (central panel) and the Λ CDM model (right panel).

this approach using the luminosity functions coming from the RDCS (Rosati et al. 1998) and BCS (Ebeling et al. 1997) samples. The result is a relation between σ_8 and the density parameter Ω_0 corresponding to the best-fit of the data to the model predictions. In order to study the dependence of our results on different choices for the normalization, we computed the clustering properties for the ABRIXAS case adopting the values of σ_8 resulting from the Borgani et al. (1999) relation, namely $\sigma_8 = 0.58, 1.00$ and 0.96 for SCDM, OCDM and Λ CDM models, respectively. The spatial correlation functions (not reported here) show differences smaller than 10 per cent with respect to those obtained with the previous normalizations. Similar differences are obtained for the other catalogues here considered.

6 CONCLUSIONS

The purpose of this paper was to present predictions for the clustering properties of X-ray selected clusters as measured in flux-limited surveys. To this aim we introduced a model which accounts for the clustering of observable objects in our past light-cone and for the redshift evolution of both the underlying dark matter covariance function and the cluster bias factor. Our approach makes use of theoretical and empirical relations between mass, temperature and X-ray luminosity of galaxy clusters which allow to translate the limiting flux of a survey (which is the observational quantity) into a corresponding minimum mass for the dark matter haloes hosting the clusters. The results of the application of this method have been found to be only slightly sensitive to the power-spectrum normalization of the cosmological models and to the parameters entering in the adopted semi-empirical relations (within a sensible range).

The model, which is able to reproduce the observed cluster counts ($\log N - \log S$) by allowing a mild redshift evolution of the temperature-luminosity relation, has been applied to obtain predictions for the two-point (spatial and angular) correlation functions and power-spectrum for present and future surveys in the framework of different cosmological scenarios. Our main results are as follows:

- In surveys with different limiting flux, the observed clusters have different properties in terms of luminosity, temperature and mass. In particular, reducing the limiting fluxes corresponds to adding smaller mass haloes. Since the bias factor is an increasing function of the mass, we find that the amplitude of the spatial correlation function of X-ray selected clusters decreases when the limiting flux is lowered. A similar conclusion has been very recently reached by Suto et al. (2000).
- We made predictions concerning different catalogues (BCS, XBACs and REFLEX) by using the actual sky coverage where available (REFLEX) and by correcting for incompleteness where necessary (XBACs). The results show that the Einstein-de Sitter models here considered always give smaller correlation amplitude compared to models with low matter density parameter, $\Omega_{\text{m}} = 0.3$.

- In the case of the XBACs catalogue, it is possible to compare our predictions with two different observational estimates (Abadi, Lambas & Muriel 1998; Borgani, Plionis & Kolokotronis 1999). As already found in a similar analysis of the RASS1 Bright Sample by Moscardini et al. (2000), only the models with low Ω_{0m} can reproduce the observed clustering, while the correlation strength for the Einstein-de Sitter models is too low.
- We applied our method also to make predictions for possible future surveys of X-ray clusters. Our results show that in subsamples of high-redshift objects the amplitude of the correlation function would be higher than the local one.
- Finally, we used our approach to discuss what would be the best strategy for future surveys, by comparing the clustering signal obtained with two different choices: a deep survey on a small area of the sky vs. a brighter survey covering a wider area. We found that the second configuration is preferable because of the size of the errorbars which would allow the detection of the clustering (both spatial and angular) on relevant scales.

In conclusion, we think that the clustering properties of X-ray selected clusters are a very powerful tool to study the large-scale structure of the universe. In fact, our results show that this approach, similarly to the study of the cluster abundances, can be successfully used to put constraints on the cosmological parameters. Such a method will become more powerful when the data for deeper surveys will be available in the next future.

ACKNOWLEDGMENTS.

This work has been partially supported by Italian MURST, CNR and ASI. We want to warmly thank Sabrina De Grandi for stimulating comments and helpful suggestions and for giving us her results about number counts at high limiting flux. We are grateful to Hans Böhringer and C. Collins for having provided the sky coverage of the REFLEX catalogue and to Stefano Borgani, Ornella Pantano, Yasushi Suto and Bepi Tormen for useful discussions. We also thank the referee, Vincent Eke, for comments which allowed us to improve the presentation of this paper.

REFERENCES

- Abadi M.G., Lambas D.G., Muriel H., 1998, *ApJ*, 507, 526
 Allen S.W., Fabian A.C., 1998, *MNRAS*, 197, L57
 Arnaud M., Evrard A.E., 1999, *MNRAS* 305, 631
 Bahcall N.A., West M., 1992, *ApJ*, 392, 419
 Bardeen J.M., Bond J.R., Kaiser N., Szalay A.S., 1986, *ApJ*, 304, 15
 Benson A.J., Cole S., Frenk C.S., Baugh C.M., Lacey C.G., 2000, *MNRAS*, 311, 793
 Böhringer H. et al., 1998, *Messenger*, 94, 21
 Borgani S., Plionis M., Kolokotronis V., 1999, *MNRAS*, 305, 866
 Borgani S., Rosati P., Tozzi P., Norman C., 1999, *ApJ*, 517, 40
 Bryan G.L., Norman M.L., 1998, *ApJ*, 495, 80
 Bunn E.F., White M., 1997, *ApJ*, 480, 6
 Carroll S.M., Press W.H., Turner E.L., 1992, *ARA&A*, 30, 499
 Catelan P., Lucchin F., Matarrese S., Porciani C., 1998, *MNRAS*, 297, 692
 Catelan P., Matarrese S., Porciani C., 1998, *ApJ*, 502, L1
 Cavaliere A., Menci N., Tozzi P., 1999, *MNRAS*, 308, 599
 Chincarini G., 1999, in *Proc. of the VLT Opening Symposium*, Springer-Verlag, in press, astro-ph/9905022
 Collins C.A. et al., 2000, in preparation
 Crawford C.S., Allen S.W., Ebeling H., Edge A.C., Fabian A.C., 1999, *MNRAS*, 306, 857
 Croft R.A.C., Dalton G.B., Efstathiou G., Sutherland W.J., Maddox S.J., 1997, *MNRAS*, 291, 305
 David L.P., Slyz A., Jones C., Forman W., Vrtilik S.D., Arnaud K.A., 1993, *ApJ*, 412, 479
 De Grandi S., Molendi S., Böhringer H., Chincarini G., Voges W., 1997, *ApJ*, 486, 738
 De Grandi S. et al., 1999a, *ApJ*, 514, 148
 De Grandi S. et al., 1999b, *ApJ*, 513, L17
 Donahue M., Voit G.M., Scharf C.A., Gioia I.M., Mullis C.R., Hughes J.P., Stocke J.Y., 1999, *ApJ*, 527, 525
 Ebeling H., Edge A.C., Böhringer H., Allen S.W., Crawford C.S., Fabian A.C., Voges W., Huchra J.P., 1998, *MNRAS*, 301, 881
 Ebeling H., Edge A.C., Fabian A.C., Allen S.W., Crawford C.S., Böhringer H., 1997, *ApJ*, 479, L101
 Ebeling H., Voges W., Böhringer H., Edge A.C., Huchra J.P., Briel U.G., 1996, *MNRAS*, 283, 1103
 Eke V.R., Cole S., Frenk C.S., 1996, *MNRAS*, 282, 263
 Eke V.R., Cole S., Frenk C.S., Henry P.J., 1998, *MNRAS*, 298, 1145
 Fisher K.B., Nusser A., 1996, *MNRAS*, 279, L1
 Frenk C.S. et al., 1999, *ApJ*, 525, 554
 Gheller C., Pantano O., Moscardini L., 1998, *MNRAS*, 296, 85
 Guzzo L. et al., 1999, *Messenger*, 95, 27
 Hamilton A.J.S., Kumar P., Lu E., Mathews A., 1991, *ApJ*, 374, L1
 Heavens A.F., Matarrese S., Verde L., 1998, *MNRAS*, 301, 797

- Henry J.P., Arnaud K.A., 1991, *ApJ*, 372, 410
Hui L., Kofman L., Shandarin S.F., 1999, preprint, astro-ph/9901104
Jain B., Mo H.J., White S.D.M., 1995, *MNRAS*, 276, L25
Jing Y.P., 1998, *ApJ*, 503, L9
Jing Y.P., 1999, *ApJ*, 515, L45
Kaiser N., 1984, *ApJ*, 284, L9
Kaiser N., 1987, *MNRAS*, 227, 1
Kauffmann G., Colberg J.M., Diaferio A., White S.D.M., 1999, *MNRAS*, 303, 188
Kitayama T., Suto Y., 1996, *ApJ*, 469, 480
Kitayama T., Suto Y., 1997, *ApJ*, 490, 557
Kravtsov A.V., Klypin A.A., 1999, *ApJ*, 520, 437
Lahav O., Fabian A.C., Edge A.C., Putney A., 1989, *MNRAS*, 238, 881
Lahav O., Lilje P.B., Primack J.R., Rees M.J., 1991, *MNRAS*, 251, 128
Liddle A.R., Lyth D.H., Roberts D., Viana P.T.P., 1996a, *MNRAS*, 278, 644
Liddle A.R., Lyth D.H., Viana P.T.P., White M., 1996b, *MNRAS*, 282, 281
Lidsey J.E., Coles P., 1992, *MNRAS*, 258, L57
Lucchin F., Matarrese S., 1985, *Phys. Rev.*, D32, 1316
Lucchin F., Matarrese S., Mollerach S., 1992, *ApJ*, 401, L49
Magira H., Jing Y.P., Suto Y., 2000, *ApJ*, 528, 30
Markevitch M., 1998, *ApJ*, 504, 27
Matarrese S., Coles P., Lucchin F., Moscardini L., 1997, *MNRAS*, 286, 115
Mathiesen B., Evrard A.E., 1998, *MNRAS*, 295, 769
Matsubara T., 1999, preprint, astro-ph/9908056
Matsubara T., Suto Y., Szapudi I., 1997, *ApJ*, 491, L1
Mo H.J., Jing Y.P., Börner G., 1992, *ApJ*, 392, 452
Mo H.J., Jing Y.P., White S.D.M., 1996, *MNRAS*, 282, 1096
Mo H.J., White S.D.M., 1996, *MNRAS*, 282, 347
Moscardini L., Coles P., Lucchin F., Matarrese S., 1998, *MNRAS*, 299, 95
Moscardini L., Matarrese S., De Grandi S., Lucchin F., 2000, *MNRAS*, in press, astro-ph/9904282
Mushotzky R.F., Scharf C.A., 1997, *ApJ*, 482, L13
Navarro J.F., Frenk C.S., White S.D.M., 1995, *MNRAS*, 275, 720
Nichol R.C., Briel O.G., Henry J.P., 1994, *MNRAS*, 267, 771
Nishioka H., Yamamoto K., 1999, *ApJ*, 520, 426
Oubkir J., Bartlett J.G., Blanchard A., 1997, *A&A*, 320, 365
Peacock J.A., Dodds S.J., 1994, *MNRAS*, 267, 1020
Peacock J.A., Dodds S.J., 1996, *MNRAS*, 280, L19
Peebles P.J.E., 1980, *The large-scale structure of the Universe*. Princeton University Press, Princeton
Peebles P.J.E., 1993, *Principles of Physical Cosmology*. Princeton University Press, Princeton
Plionis M., Kolokotronis V., 1998, *ApJ*, 500, 1
Ponman T.J., Bourner P.D.J., Ebeling H., Böhringer H., 1996, *MNRAS*, 283, 690
Porciani C., 1997, *MNRAS*, 290, 639
Porciani C., Catelan P., Lacey C., 1999, *ApJ*, 513, L99
Postman M., 1998, in *Banday A.J., Sheth R.K. & L.N. da Costa eds., Proc. of MPA/ESO Conference on Evolution of Large Scale Structure: from Recombination to Garching*, in press, astro-ph/9810088
Press W.H., Schechter P., 1974, *ApJ*, 187, 425
Romer A.K., Collins C.A., Böhringer H., Cruddace R.C., Ebeling H., MacGillawray H.T., Voges W., 1994, *Nat*, 372, 75
Rosati P., Della Ceca R., Norman C., Giacconi R., 1998, *ApJ*, 492, L21
Sadat R., Blanchard A., Oubkir J., 1998, *A&A*, 329, 21
Schuecker P. et al., 2000, in preparation
Sheth R.K., Mo H.J., Tormen G., 1999, preprint, astro-ph/9907024
Sheth R.K., Lemson G., 1999, *MNRAS*, 304, 767
Sheth R.K., Tormen G., 1999, *MNRAS*, 308, 119
Sugiyama N., 1995, *ApJS*, 100, 281
Suto Y., Magira H., Jing Y.P., Matsubara T., Yamamoto K., 1999, *Prog. Theor. Phys. Suppl.*, 133, 183
Suto Y., Yamamoto K., Kitayama T., Jing Y.P., 2000, *ApJ*, in press, astro-ph/9907105
Sutherland W.J., 1988, *MNRAS*, 234, 159
Taylor A.N., Hamilton A.J.S., 1996, *MNRAS*, 282, 767
Trümper J., Hasinger G., Staubert R., 1998, *AN*, 319, 113
Viana P.T.P., Liddle A.R., 1996, *MNRAS*, 281, 323
Viana P.T.P., Liddle A.R., 1999, *MNRAS*, 303, 535
Voit G.M., Donahue M., 1998, *ApJ*, 500, L111
White D.A., Jones C., Forman W., 1997, *MNRAS*, 292, 419
White M., Gelmini G., Silk J., 1995, *Phys. Rev.*, D51, 2669
White M., Viana P.T.P., Liddle A.R., Scott D., 1996, *MNRAS*, 283, 107
Yamamoto K., Nishioka H., Suto Y., 1999, 1999, 527, 488
Yamamoto K., Suto Y., 1999, *ApJ*, 517, 1
Zaroubi S., Hoffman Y., 1996, *ApJ*, 462, 25